



بسم الله الرحمن الرحيم

# Sudan University of Science and Technology College of Graduate Studies

## Effect of Energy and Number of Laser Pulses on the Optical Properties of ZnS Thin Films Prepared By Pulse Laser Deposition Technique

تأثير طاقة وعدد نبضات الليزر علي الخصائص البصرية لأغشية كبريتيد الزنك الرقيقة  
المحضرة باستخدام تقانة الترسيب بالليزر النبضي

A Thesis Submitted in Fulfillment of the Requirements for the Degree of Doctor of Philosophy in  
Laser Applications in Physics

**By:**

Mohammed Nouman Mohamed Abd Alla

**Supervised by:**

Dr. Khalid Mohammed Haroun Mohammed

March 2019

## الاية

قال تعالى:

(الله لا اله الا هو الحي القيوم لا تاخذه سنة ولا نوم له ما في السموات و ما في الارض من ذا الذي يشفع عنده الا باذنه يعلم ما بين ايديهم وما خلفهم ولا يحيطون بشئ من علمه الا بما شاء وسع كرسيه السموات والارض ولا يؤوده حفظهما وهو العلي العظيم)

صدق الله العظيم

سورة البقرة (اية 255)

## **Dedication**

*I dedicate this work to My family members, especially my work is dedicated to the Souls of My “**Father** “,, and to my **Mother**, who always support and encourage me to go forward. Also my work is dedicated to my lovely sisters and my **Brothers***

*My work is dedicated also to my small family,, my lovely wife **Sarah Salih Badry** she was patient with me, she was helped me and organize my life. She was keeping my note sheets that I was wrote during the course of this study... To the beautifully thing that I have in my life my Sons "**Nouman**", **Salih**", "**Mustafa**", and **Yousif**" and to the One's whom comes after insha Allah.*

*I also dedicate my work to my colleagues.*

*To everyone whom encourage, advice or help me during my whole university studies from undergraduate to the PhD level.*

## **Acknowledgement**

First of all thanks a lot to Allah who give me the power and health to complete this work. Firstly I would like to thanks m **Dr. Khalid Mohamed Haroun**, it would have been very difficult for me to complete this thesis without the kind support and helps that he gave to me. I express my deep sense of gratitude for his excellent guidance, competent advice, keen observations and persistent encouragement as well as personal attention given to me during the entire course of work. I learned more from him, he was and will be the best teachers that I met during my whole studies and I wish to him all the best things. Finally, no amount of words can adequately express the debt I owe to him. I wish to defense this work under his supervision.

I would like to extend deep gratitude to **Dr. Ali Abd Alrahman Marouf**, and **Dr. Sohad Saad Elwakeel** of the Laser Institute, Sudan University of Science & Technology whom helped advice, encouraged and supports me

Also I would like to express my deepest thanks to **Dr. Yousif Hassan Alsheikh** of the Omdurman Ahlia University, for his continuous support.

With a sense of gratitude, I am thankful to all the office and library staff of the institute of laser –Sudan University of Science and Technology and the technical staff for all the help and cooperation.

## Abstract

The field of this research was thin films fabrication using pulse laser deposition technique. The aim of this work is to study the effect of the laser parameters (number of pulses and laser pulse energy) on the optical properties of the ZnS thin films fabricated by pulsed laser deposition technique. Eight Samples of ZnS thin films were fabricated by using Q-Switched Nd: YAG laser with the fundamental wavelength of 1064 nm, four of the samples were fabricated using different number of pulses (10, 15, 20, and 25) with 100 mj pulse energy and 2 Hz pulse repetition rate, the other four samples were fabricated using laser pulse energies of (125, 150, 175, and 200) mj with fixed number of pulses of 20, and pulse repetition rate of 5 Hz. The target to the substrate distance and angle were kept fixed, 2 cm, and 45° respectively. The film thicknesses were measured using FESEM measurement tool. The results showed that for the case of changing the number of laser pulses, the transmission spectra in the region (532 to 915) nm were found to be in the range from 0.40 to 0.62% depending on the ZnS thin film thickness and for each ZnS thin film the transmission spectrum is unique., and the absorption coefficients were found to be varied from (28.287 to 7.300) \*10<sup>3</sup> cm<sup>-1</sup> depending on the film thickness and wavelength. And for the case of fabricating the thin films using varied pulse energy, the thickness of the deposited ZnS thin films was found to be increased when pulse energy is increased. The transmission spectra in the tested region (532 to 915) nm were found to be in the range from 0.41 to 0.59 % depending on the ZnS thin film thickness, and for each ZnS thin film the transmission spectrum is unique. The refractive indices of all samples were found to be (2.51 lower and 3.38 higher) and change with the thin film thickness and with the wavelengths. Transmission spectra, absorption coefficients and the refractive indices of all samples they were in good agreement with the literature.

## المستخلص

يعد هذا البحث ضمن مجال تصنيع الاغشية الرقيقة المصنعة بتقانة الترسيب بالليزر النبضي. يهدف هذا البحث لدراسة اثر معاملات الليزر ( عدد نبضات وطاقة النبضة) على الخصائص البصرية لاغشية كبريتيد الزنك الرقيقة المحضرة بتقانة الترسيب بالليزر النبضي.

صنعت ثمانية عينات من اغشية كبريتيد الزنك الرقيقة باستخدام ليزر نيوديوم ياك ذو التشغيل المفتاحي ذو الطول الموجي 1064 نانومتر، حيث صنعت اربعة من العينات باستخدام عدد نبضات مختلف (10، 15، 20، و 25) بطاقة نبضة 100 ميلي- جول و2 هيرتز معدل تكرار النبضات، والاربعه عينات الاخرى صنعت باستخدام طاقات مختلفة لنبضة الليزر (125، 150، 175، و 200) ميلي – جول بعدد نبضات ثابت من 20 نبضة وعدد تكرار للنبضات 5 هيرتز. حيث كانت المسافة والزاوية بين الهدف والركيزة ثابتة عند 2 سم و45 درجة على التوالي. حيث تم قياس سماكات الاغشية الرقيقة المصنعة باستخدام المجهر الالكتروني الماسح الباعث للمجال (FESEM). واوضحت النتائج في حالة تغيير عدد نبضات الليزر ان اطياف النفاذية في المدى ( 532 الي 915) نانومتر لكل غشاء رقيق تتراوح بين (0.4% و0.62%) اعتمادا على سمك غشاء كبريتيد الزنك الرقيق وان لكل غشاء رقيق طيف نفاذية متفرد. وان معاملات الامتصاص تتراوح بين (7.300 و 28.287) \* $10^{-3}$  سم<sup>-1</sup> اعتمادا على سمك الغشاء والطول الموجي. اما في حالة تصنيع الاغشية الرقيقة عن طريق تغيير طاقة نبضة الليزر وجد ان سمك غشاء كبريتيد الزنك المصنع يزداد بزيادة طاقة النبضة المستخدمة. ان اطياف النفاذية في المدى ( 532 الي 915) نانومتر لكل غشاء رقيق تتراوح بين (0.41% و 0.59%) اعتمادا على سمك الغشاء ولكل غشاء طيف نفاذية متفرد. وكذلك وجد ان معاملات الانكسار ( ادنى 2.51 و 3.38 اعلى) لكل العينات و تتغير بتغير سمك الغشاء والطول الموجي. ووجد ان اطياف النفاذ، معاملات الامتصاص ومعاملات الانكسار لكل العينات تتفق مع الدراسات السابقة .

## Table of Contents

Title	Page
الإية	<b>i</b>
Dedication	<b>ii</b>
Acknowledgement	<b>iii</b>
Abstract	<b>iv</b>
المستخلص	<b>vi</b>
List of Figures	<b>xii</b>
List of Tables	<b>xvi</b>
List of Abbreviations	<b>xvii</b>
<b>CHAPTER ONE BASIC CONCEPTS</b>	
1- 1 Introduction:	<b>1</b>
1-2 Problem statement:	<b>3</b>
1-3 Research Methodology:	<b>3</b>
1-4 Research Objectives:	<b>4</b>
1-5 Research Outlines:	<b>4</b>
<b>CHAPTER TWO THIN FILMS AND PULSED LASER DEPOSITION</b>	
2-1 Introduction:	<b>5</b>
2-2 Basics of thin films:	<b>5</b>
2.2.1 Single layer:	<b>5</b>
2.2.2 Multilayer thin films:	<b>6</b>
2.2.3 Spectroscopy:	<b>6</b>
2-3 Film growth modes:	<b>7</b>
2.4 Thin film properties:	<b>9</b>
2.4.1 The Physical properties:	<b>10</b>
2.4.1.1 Thickness of the film:	<b>11</b>

2.4.2 Optical Properties:	12
2.5 Applications of thin films:	13
2.6 Deposition techniques	14
2.6.1 Chemical methods:	14
2.6.2 Physical methods:	15
2.6.2 .1 Diode Sputtering	18
2.6.2.2 Reactive Sputtering	18
2.6.2. 3. Bias Sputtering	18
2.6.2. 4. Magnetron Sputtering	19
2.6.2 .5. Ion-Beam Sputtering	20
2.6.3 Pulsed laser deposition:	20
2.6.3.2 Basics of PLD	21
2.6.3.2 Mechanisms of PLD	23
2.6.3.3 Advantages of PLD:	26
2.6.3.4 Disadvantages of PLD:	28
2.7 Laser ablation and plasma formation:	30
2.7.1 Expansion of the plasma plume in vacuum:	31
2.7.2 Expansion of the plasma plume into background gas:	32
2.8 Lasers for infrared laser ablation and deposition:	32
2.9 Deposition parameters:	33
2.10 Literature Review:	33
<b>CHAPTER THREE EXPERIMENTAL PART</b>	
3-1 Introduction:	43
3-2 Materials used:	43



3-2-1 Potassium bromide (KBr):	<b>43</b>
3-2-2 Zinc Sulphide (ZnS):	<b>44</b>
3-2-2-1 ZnS properties:	<b>45</b>
3-2-2-2 Applications of ZnS:	<b>46</b>
3-3 Target preparation, machine and method:	<b>47</b>
3-4 Substrates:	<b>47</b>
3-5 The Q-Switched Nd: YAG laser source:	<b>47</b>
3-4-1 Q-switched Nd: YAG (OW-D1 model) specifications:	<b>49</b>
3-4-2 Advantages:	<b>50</b>
3-5 Field Emission Scanning Electron microscope:	<b>50</b>
3-5-1MIRA3 key feature:	<b>53</b>
3-5-2 The FESEM MIRA3 stage and the sample holder:	<b>53</b>
3-6 Methodology of ZnS thin films deposition and characterization:	<b>54</b>
<b>CHAPTER FOUR</b>	
<b>RESULTS AND DISCUSSION</b>	
4-1 Introduction:	<b>58</b>
4-2 Number of Pulses Influences thickness and optical properties of ZnS thin films:	<b>58</b>
4-3 Effect of Pulse Energy on the thickness and Optical properties of ZnS thin films:	<b>70</b>
4-4 Discussion:	<b>81</b>
4-5 Conclusions:	<b>83</b>
4-6 Recommendations:	<b>84</b>
References:	<b>85</b>
Appendices:	<b>91</b>

## List of Figures

Figure title	Page
Figure 2.1: Single layer thin film	6
Figure 2.2: Multilayer thin film structure	6
Figure 2.3: Schematic diagram of atomic processes in the nucleation of three dimensional clusters of deposited film atoms on a substrate surface.	7
Figure 2.4: Schematic representation of different growth modes. $\Theta$ is the coverage of film material in units of monolayer's	8
Figure 2.5: Evaporation setup	17
Figure 2.6: Most useful thin film deposition methods	17
Figure 2.7: PLD setup	23
Figure 2.8: plasma- substrate interaction	25
Figure 3.1: transmission spectrum of the KBr	44
Figure 3.2: The ZnS structure	46
Figure 3.3: User interface of Q-Switched Nd: YAG laser source model OW-D1	48
Figure 3.4: Schematic diagram of the scanning electron microscope	51
Figure 3.5: A photograph of the FESEM, shown	52
Figure 3.6: FESEM stage and sample holder	54
Figure 3.7: The experimental setup for fabrication of ZnS thin films	55
Figure 3.8: Diagram of the experimental setup for optical measurement of ZnS thin films	56
Figure (4.1, a): FESEM image of ZnS thin film deposited on glass substrate with 10 laser pulses, laser pulse energy of 100 mj and repetition rate of 2 Hz	59
Figure (4.1, b): FESEM image of thickness measurement of ZnS thin film deposited on glass substrate with 10 laser pulses, laser pulse energy of 100 mj and repetition rate of 2 Hz	59
Figure (4.2, a): FESEM image of ZnS thin film deposited on glass substrate with 15 laser pulses, laser pulse energy of 100 mj and repetition rate of 2 Hz	60
Figure (4.2, b): FESEM image of thickness measurement of ZnS thin	60

film deposited on glass substrate with 15 laser pulses, laser pulse energy of 100 mj and repetition rate of 2 Hz	
Figure (4.3, a): FESEM image of ZnS thin film deposited on glass substrate with 20 laser pulses, laser pulse energy of 100 mj and repetition rate of 2 Hz	<b>61</b>
Figure (4.3, b): FESEM image of thickness measurement of ZnS thin film deposited on glass substrate with 20 laser pulses, laser pulse energy of 100 mj and repetition rate of 2 Hz	<b>62</b>
Figure (4.4, a): FESEM image of ZnS thin film deposited on glass substrate with 25 laser pulses, laser pulse energy of 100 mj and repetition rate of 2 Hz	<b>62</b>
Figure (4.4, b): FESEM image of thickness measurement of ZnS thin film deposited on glass substrate with 25 laser pulses, laser pulse energy of 100 mj and repetition rate of 2 Hz	<b>63</b>
Figure (4.5): The ZnS thin film thicknesses versus the number of laser pulses used for deposition	<b>64</b>
Figure (4.6): Transmission spectra of the four ZnS thin film samples deposited using different number of laser pulses	<b>66</b>
Figure (4.7): The refractive indices of the four samples of ZnS thin films versus wavelengths as a function of the number of laser pulses	<b>68</b>
Figure (4.8): Absorption coefficients versus wavelengths for four samples of ZnS thin films as a function of the number of laser pulses	<b>69</b>
Figure (4.9, a): FESEM image of ZnS thin film deposited on glass substrate with laser pulse energy of 125 mj and repetition rate of 5 Hz	<b>70</b>
Figure (4.9, b): FESEM image of thickness measurement of ZnS thin film deposited on glass substrate with laser pulse energy of 125 mj and repetition rate of 5 Hz	<b>71</b>
Figure (4.10, a): FESEM image of thickness measurement of ZnS thin film deposited on glass substrate with laser pulse energy of 150 mj and repetition rate of 5 Hz	<b>71</b>
Figure (4.10, b): FESEM image of thickness measurement of ZnS thin film deposited on glass substrate with laser pulse energy of 150 mj and repetition rate of 5 Hz	<b>72</b>
Figure (4.11, a): FESEM image of thickness measurement of ZnS thin	<b>73</b>

film deposited on glass substrate with laser pulse energy of 175 mj and repetition rate of 5 Hz	
Figure (4.11, b): FESEM image of thickness measurement of ZnS thin film deposited on glass substrate with laser pulse energy of 175 mj and repetition rate of 5 Hz	<b>73</b>
Figure (4.12, a): FESEM image of thickness measurement of ZnS thin film deposited on glass substrate with laser pulse energy of 200mj and repetition rate of 5 Hz	<b>74</b>
Figure (4.12, b): FESEM image of thickness measurement of ZnS thin film deposited on glass substrate with laser pulse energy of 200 mj and repetition rate of 5 Hz	<b>74</b>
Figure (4.13): The relation between laser pulse energy ZnS thin film thickness	<b>75</b>
Figure (4.14): Transmission spectra of the four ZnS thin film samples deposited using different laser pulse energy	<b>77</b>
Figure (4.15): Refractive indices of the four ZnS thin film samples deposited using different laser pulse energy	<b>78</b>
Figure (4.16): Absorption coefficients versus wavelengths for four samples of ZnS thin films deposited using different pulse energy	<b>80</b>

## List of Tables

Table title	Page
Table 3.1: the most important properties of the ZnS:	<b>45</b>
Table 3.2: Specifications of the Q-switched Nd: YAG laser source:	<b>49</b>
Table 3.3: the laser sources used for transmission spectra measurement:	<b>56</b>
Table 4.1: Thicknesses of the four fabricated ZnS thin films versus number of laser pulses:	<b>64</b>
Table 4.2: Transmission percentages at certain wavelengths for four ZnS thin films	<b>65</b>
Table 4.3: Refractive indices of the four ZnS thin film samples deposited with different number of laser pulses:	<b>67</b>
Table 4.4: Absorption coefficients of the four ZnS thin film samples deposited with different number of laser pulses:	<b>69</b>
Table (4.5): Laser pulse energy against ZnS thin film thickness	<b>75</b>
Table (4.6): Transmission of the four ZnS thin films deposited using different laser pulse energy:	<b>76</b>
Table (4.7): Refractive index of the four ZnS thin films deposited using different laser pulse energy:	<b>78</b>
Table 4.8: Absorption coefficients of the four ZnS thin film samples deposited using different laser pulse energy:	<b>79</b>

## List of Abbreviations

Abbreviation	Stands for
AFM	Atomic Force Microscopy
APCVD	Atmospheric-Pressure Chemical Vapor Deposition
A. R .	Anti-reflection
ARE	Activated Reactive Evaporation
CBD	Cluster beam deposition
CAAC	C-Axis-Aligned Crystalline
CDW	Charge Density Wave
CVD	Chemical Vapor Deposition
CW	Continuous Wave
EDX	Energy Dispersive X-Ray
EBSD	Electron back scatter diffraction
GLAD	Glancing Angle Deposition
GMR	Giant Magneto-Resistance
FESEM	Field Emission Scanning Electron Microscope
Fig.	Figure
Fs	Femtosecond
HTS	High-Temperature Superconducting
IB	Inverse Bremsstrahlung
IGZO	Indium Gallium Zinc Oxide
IML	Intermediate Lens
LA-ICP-MS	Laser-Ablation Inductively Coupled Plasma Mass Spectrometry
LIBS	Laser-Induced Breakdown Spectroscopy
LPCVD	Low Pressure Chemical Vapor Deposition
MBE	Molecular-Beam Epitaxy
MOCVD	Metal Organic Chemical vapor deposition
PEPLD	Plasma-Enhanced Pulsed Laser Deposition
PHCVD	Photo –Enhanced Chemical Vapor Deposition
PLD	Pulse Laser Deposition
PVD	Physical Vapor Deposition
RHEED	Reflection High Energy Electron Diffraction
SEM	Scanning Electron Microscopy
SIMS	Secondary Ion Mass Spectroscopy
TEM	Transmission Electron Microscopy
XAS	X-ray Absorption Spectroscopy

XRD

**X-Ray Diffraction**

XPS

**X-ray Photoemission Spectroscopy**

---

# CHAPTER ONE

## BASIC CONCEPTS

### 1-1 Introduction:

The beginning of “Thin Film Science” can possibly be traced to the observations of Grove who noted that metal films were formed by sputtering of cathodes with high energy positive ions (Ghosh, D. S., 2013). The phenomenal rise in thin film researches is no doubt due to their extensive applications in the diverse fields of electronics, optics, space science, aircrafts, defense and other industries (MC RAO, 2013). Advances in thin film deposition techniques during the 20th century have enabled a wide range of applications in different areas such as magnetic recording media, electronic semiconductor devices, LEDs, optical coatings, hard coatings on cutting tools, and for both energy generation (e.g. thin-film solar cells) and storage (thin film batteries). Some of the factors which determine the physical, electrical, optical and other properties of thin film – such as rate of deposition, substrate temperature, environmental conditions, gas pressure in the system, purity of the material, inhomogeneity of the film, structural and compositional variations of the film etc. are very important. In addition to their applied interest, thin films play an important role in the development and study of materials with new and unique properties. Two dimensional materials (i.e. thin film) such as  $\text{MoS}_2$  have been the main focus of intense research efforts over the past few years. The most common method of exfoliating these materials, although efficient for lab-scale experiments, is not acceptable for large area and practical applications (Serna, Martha I. et al., 2016).

Sulphur compounds such as CdS, ZnS are an important II–VI compound semiconductor material with applications in several heterojunction photovoltaic systems and they have also applications in various electro-optic and infrared devices.



Most sulphur compounds with wide band gap which is suitable for applications in solar cells, solar selective decorative coatings, UV light emitting diode, photocatalysis and phosphors in flat panel displays (Anuar Kassim, et al., 2010). These materials when fabricated in thin film structure their properties can be tailored example are CdS (F. Lisco, et al., 2015). Thin films of sulphur compounds are non-toxic to human body, very cheap and abundant (Anuar Kassim, et al., 2010). Many methods were used to deposit thin film materials they are either pure physical or pure chemical. Physical methods contain evaporation and sputtering methods each of them can have a large numbers of deposition techniques, for example, thermal evaporation method, electron beam evaporation method, pulsed laser deposition can all be classified as physical evaporation techniques. The beauty of Pulsed Laser Deposition as a thin film growth technique is its conceptual simplicity. Ever since the discovery of the first lasers in the 1960s, this technique has undergone tremendous development, and is now applicable for the deposition of a wide range of materials, from thin polymer films to superconductors, complex oxides, metals, biomaterials and many more . Complete deposition systems can be bought, both for research purposes and large scale thin film manufacturing. PLD is a cheap and practically simple thin film deposition method, growing in popularity (Carl Philip, 2014). ZnS thin films are believed to be one of the most promising materials for blue light emitting diodes, and in electroluminescent displays, and many other applications (M. H. Suhail and R. A. Ahmed 2014). Zinc Sulphide (ZnS) is a wide gap and direct transition semiconductor that belong to group II-VI semiconductors (K. R. Murali, 2014). As a result, ZnS is an important material used as an antireflection coating in heterojunction solar cells and in infrared windows (J. Mohamed, 2002). Many methods can be used to produce thin films from this material such as sol-gel, radiofrequency sputtering [6], pulse laser deposition (Kumar V et al., 2015); (N. A. Almuslet, Kh. Haroun and Y. Alsheikh, 2018 ) and so on. Pulse laser deposition (PLD) has been successfully used to deposit an extraordinary wide range (Mohammed A. Hameed,

2015). In thin films fabricated using PLD method a number of deposition conditions corresponds to the properties of the laser beam such as laser wavelength, laser pulse energy, pulse repetition rate, etc., together with the other pulsed laser deposition conditions such as substrate temperature, ambient gas and pressure, target to substrate distance and angle are all considered as fundamental thin film depositions conditions that controlled the properties of the deposited thin films .The PLD is widely used technique for the fabrication of thin films because of its numerous advantages such as its simplicity, etc (Yousif H. Alsheikh, 2018). The PLD technique enables the deposition of many complex materials over a wide range of background gas composition and pressures. Throughout this chapter the research objectives, problem statement, and research methodology will be given.

## **1-2 Problem statement:**

There is a need to investigate the properties of the ZnS thin films deposited using pulse laser deposition technique, and to study the effect of the properties of the laser properties (laser pulse energy and the number of the laser pulses) on the thickness and optical properties of the ZnS deposited films.

## **1-3 Research Methodology:**

The experimental deposition of the ZnS thin films using different laser pulse energy and using different number of the laser pulses on glass substrates by using Q-Switched Nd: YAG laser source, and then each fabricated ZnS thin film will be imaged and its thickness will be measured using the Field Emission Scanning Electron Microscope (FESEM). Then each the transmission of each ZnS thin film will be detected and measured at certain monochromatic wavelengths and after recording the transmission spectra of the ZnS thin films together with their thicknesses measured will be used to calculate their optical properties (refractive index, absorption coefficients) will be the methodology of this research.

## **1-4 Research Objectives:**

The objectives of this work are:

- Using the pulse laser deposition method to produce thin films of some sulphur compounds typically ZnS on different glass substrates.
- Studying the optical properties of the produced thin films.
- Studying the effect of laser parameters (pulse energy, and the number of the laser pulses) on the thickness and optical properties of the produced films.

## **1-5 Research Outlines:**

This chapter presents an introduction, research objectives, and basics of thin films, deposition methods, thin film properties and thin film applications. Chapter two describes in details the basic principles underlined the pulsed laser deposition and discuss the pulsed laser deposition advantages and disadvantages and at the end of the chapter literature review is presented. Experimental part of this work including materials and tools, in addition to the methodology followed to produce the thin films and the method for determination of the optical properties of the produced films are presented in chapter three. Finally chapter four includes the results and discussion, conclusion and recommendation for future works.

# CHAPTER TWO

## THIN FILMS AND PULSED LASER DEPOSITION

### 2-1 Introduction:

This chapter describes in details the field of thin film, types, methods of preparation, and applications and only describe the optical properties of thin film material since it's vital for the thesis, also the chapter discusses in details the Pulsed-laser deposition (PLD) is one of the most promising techniques for the formation of complex-oxide heterostructures, superlattices, and well-controlled interfaces. In this chapter the basic mechanisms of the PLD and at the end of this chapter literature works in the field are reviewed

### 2-2 Basics of thin films:

A thin film is a layer of material ranging from fractions of a nanometer (monolayer) to several micrometers (5 micrometers) in thickness. A material with thickness greater than the upper limit thickness of thin film up to 500 microns is said to be thick film. Above than 500 microns the material is entering the Bulk structure classification. Thin films are classified in many ways, mainly , according to the materials used for the coatings, number of layers, the damage threshold, the strength , and the characteristics, etc. there are metallic coating , and dielectric coatings .The metallic coating always have lot of absorption and have only limited applications. According to the number of deposited layers there are:

#### 2.2.1 Single layer:

This is a type of thin film in which only single layer is deposited into a substrate, such as illustrated in figure (2.1) below:

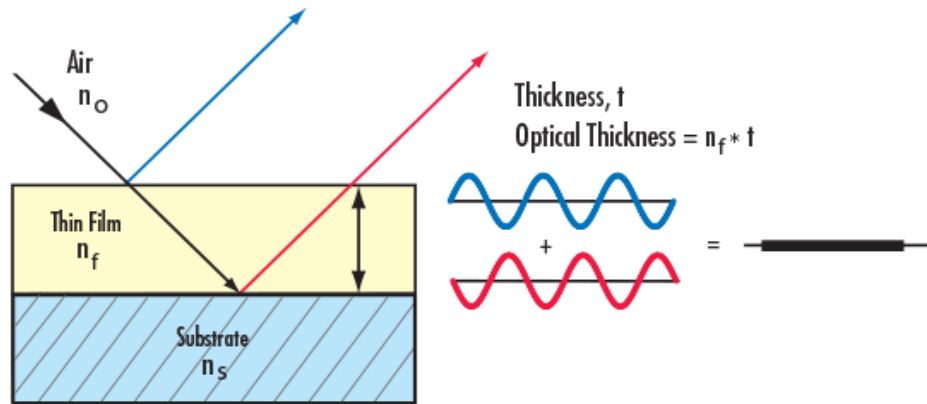


**Figure 2.1: Single layer thin film**

### 2.2.2 Multilayer thin films:

This is a type in which  $n$  layers (stack) are deposited into a substrate; multilayer thin films find a wide range of applications in solar energy, semiconductor devices and so on. Figure 2.2 shows a diagram of multilayer thin film structure.

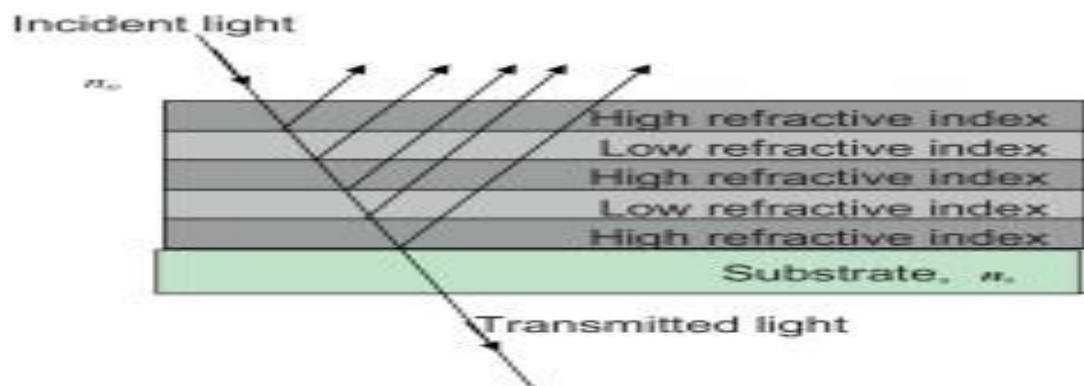


**Figure 2.2: Multilayer thin film structure**

### 2.2.3 Spectroscopy:

There is a connection between the fabrication of thin films and their optically characterization through the science of spectroscopy. So to study the optical properties such as the thin film refractive index, the absorption coefficients, the transmission, and so on for the thin films a variety of techniques can be used. Spectroscopy is the study of the absorption and emission of light and other radiation by matter, as related to the

dependence of these processes on the wavelength of the radiation. Optical spectroscopy is used routinely to identify the chemical composition of matter and to determine its physical structure. Spectroscopic techniques are extremely sensitive. Single atoms and even different isotopes of the same atom can be detected among  $10^{20}$  or more atoms of a different species. Trace amounts of pollutants or contaminants are often detected most effectively by spectroscopic techniques. Certain types of microwave, optical, and gamma-ray spectroscopy are capable of measuring infinitesimal frequency shifts in narrow spectroscopic lines. Frequency shifts as small as one part in  $10^{15}$  of the frequency being measured can be observed with ultrahigh resolution laser techniques. Because of this sensitivity, the most accurate physical measurements have been frequency measurements (Zarrin Es'haghi, 2011).

### **2-3 Film growth modes:**

Depending on many factors, the thin film growth modes are important to study for one working on thin film technology. The different processes involved in the nucleation of clusters on a surface by vapour deposition of atoms are shown in figure (2-3). Film atoms arrive at a rate dependent on the deposition parameters either on bare substrate areas or on preexisting clusters of film atoms. These film atoms can subsequently diffuse over the substrate or cluster surface, encounter other mobile film atom to form mobile or stationary clusters, attach to preexisting film-atom clusters, be re-evaporated from the substrate or from a cluster, or be detached from a cluster and remain on the substrate surface.

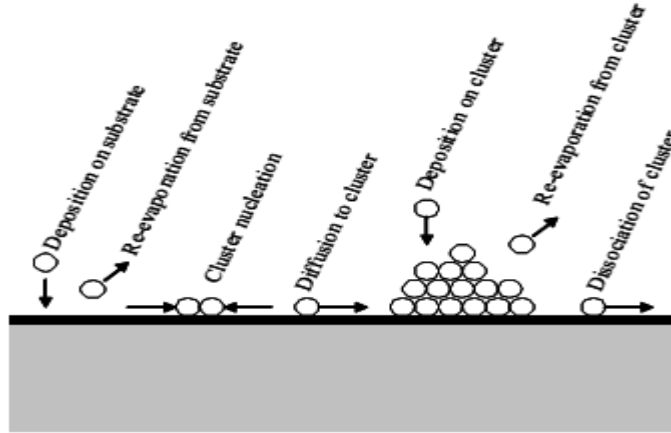


**Figure 2.3: Schematic diagram of atomic processes in the nucleation of three dimensional clusters of deposited film atoms on a substrate surface.**

The film growth modes are typically of three types,

**a- Layer type:**

Full monolayer growth involves the nucleation and growth of islands that are only one monolayer thick and grow to essentially complete coalescence before significant clusters are developed on the next film layer. In this case there is no free energy barrier to nucleation, i.e. no  $\Delta G^*$ . If the substrate material is different from the film material, full monolayer nucleation will be promoted by strong film-substrate bonding, low film surface energy and high substrate surface energy.

**b- Mixed type:**

Full monolayer growth may change to three-dimensional island growth after 1-5 monolayer's due to a change in the energy situation with successive monolayer's. This might be an increase in stress with increasing layer thickness due to mismatched lattice spacing's. These three growth types are illustrated in figure (2-4).

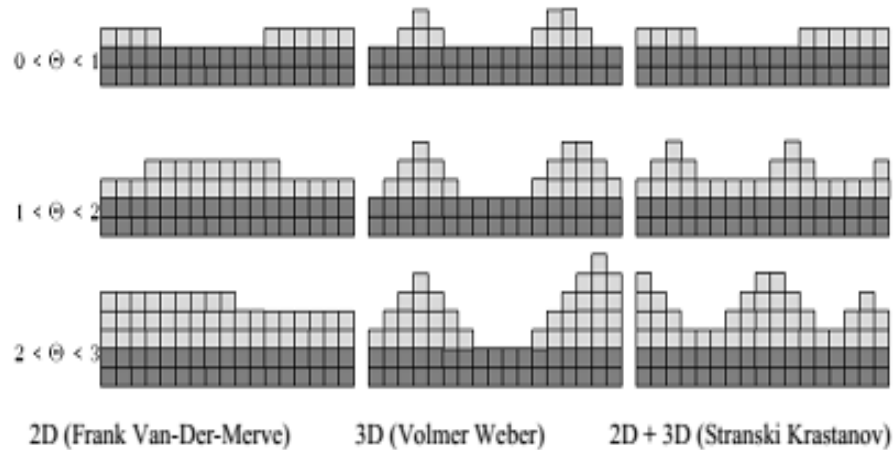


**Figure 2.4: Schematic representation of different growth modes.  $\Theta$  is the coverage of film material in units of monolayer's**

The selection of one of these growth modes by a substrate-film system depends on: (a) the thermodynamics that relates the surface energies of the film and substrate, and (b) the film substrate interface energy.

## 2.4 Thin film properties:

The properties of thin films are sensitive to the method of preparation.

Therefore to make sure that the thin film which was produced by a given process satisfy the specified technological demands, a wide field of characterization, measurement and testing methods are available (Davis, Peter L. et al., 2015). The physical properties of a thin film are highly dependent on their thickness. The determination of the film thickness and of the deposition rate, therefore, is an important issue in the thin film technology. In many applications it is necessary to have a good knowledge about the current film thickness even during the deposition process, as for example in the case of optical coatings. Therefore, one distinguishes between thickness measurement methods which are applied during deposition ("in situ") and methods by which the thickness can be determined after finishing a coating run ("ex situ"). Nonetheless, the desired mechanical, optical, chemical or electronic properties are often



opposed to the bulk properties which may be high mechanical stability, easy manufacturing or low material cost (Yousif H. Alsheikh, 2018).

The most important properties are:

#### **2.4.1 The Physical properties:**

Numerous studies have been carried out investigating processes to create thin films, characterize them, and test their physical properties (Zhao, Y.P. and Wang, T.M Lu, 2001). The beautifully hierarchical complexity associated with thin film microstructure and surface morphological evolution, which arises from a diverse set of competitive kinetic instabilities, operating on very different time and length scales, assures that thin film nanoscience and technology will remain a vital and exciting field long into the future. One may obtain a wide variety of different surface/interface morphologies and film microstructure which are inherently related to dynamic growth mechanisms. These, in turn, have a significant and generally different influence on physical properties. Although epitaxial growth of a film in the layer-by-layer mode can commence in some cases within a certain temperature regime, such a growth mode may not always occur and instead growth front can be rough in the form of mounds (multilayer step structure; unstable growth) or due to noise induced roughening during the growth can lead to the formation of self affine fractal morphologies. Besides kinetic effects during growth, stress relaxation in between film interfaces strongly alters growth characteristics and has to be taken certainly into consideration (Yousif H. Alsheikh, 2018).

##### **2.4.1.1 Thickness of the film:**

One important factor that has a principal effect on the characteristics of a work piece is the thickness of the fabricated film. Optical techniques for film-thickness determinations are widely used because they are applicable to both opaque and transparent films and generally yield thickness values of high accuracy (Almuslet

and Alsheikh, 2015); (Hernández M. et al.,1999). The thicknesses of deposited material defines its type, for thickness of the range 1 microns and down to a couple of nanometers the structure is known as thin film whereas the range of thicknesses from above 1 micron up to 500 microns the structure is said to be thick film. Since the thickness affects the optical properties of materials these two types of structure may have different optical properties due to thickness differences. Optical properties of thin and thick films such as transmittance, absorptance and reflectance in addition to the optical constants are different for the two film structures. Optical constants are parameters which characterize how a material will respond to excitation by an electromagnetic field at a given frequency, optical constants  $n$  and  $k$  represent the optical properties of a material in terms of how the electromagnetic waves propagate in that material. It should note that there can be very significant differences between optical constants measured from a bulk specimen of a material and the optical constants of a thin film of the same material. This is primarily related to the micro-structural differences in the film, but can also due to size effects to very thin films. The optical constants of all materials have some sort of expected dispersion as a function of wavelength. Optical constants of real materials, however, are not random functions of wavelength. There are generally smooth functions of wavelength and there is causality relationship between real and imaginary parts. Because of this, the optical constants for many materials can be very accurately modeled using functional forms. Thickness of the thin film is an important parameter that has to be taken into account when fabricating a thin film for specific applications. The thinness of the film is an important factor that controls the physical properties of the thin film. Controlling the thickness of the thin film will lead to control of the structural, optical and electrical properties of the films, and so on. For example optical transmission, reflection, and absorption of a thin film of a given material are highly dependent on its thickness. This a direct relation between the thin film thickness and its optical properties are clear

when considering the mathematical equation of Beer-Lambert law and spectroscopic relations of the optical transmission and absorption coefficient for the case of thin films. Whereas the dependence of the electrical and structural properties of the thin film on its thickness can be seen in the same way as with the dependence of the optical properties of the thin film on its thickness. It is interesting to notice that current trends in the industry are to produce components, e.g. as microchips having non-uniform exterior surfaces but require to be covered by uniform coatings (Daniele Dipresa, 2013).

#### **2.4.2 Optical Properties:**

Optical properties of a material change or affect the characteristics of light passing through it by modifying its propagation vector or intensity. The study of optical properties of thin films has special significance in the world of science, technology and industry for the development of new optical devices. Optical absorption study of materials provides useful information to analyze some features concerning the band structure of materials (Yousif H. Alsheikh, 2018). The optical band gap energy of the semiconductor is an important parameter that plays a major role in the construction of photovoltaic cells ( A. U. Ubale et al., 2012). Two of the most important optical properties are the refractive index  $\mathbf{n}$  and the extinction coefficient  $\mathbf{K}$ , which are generically called optical constants; though some authors include other optical coefficients within this terminology. The latter is related to the attenuation or absorption coefficient  $\alpha$  (J. Singh, 2006). The optical constants of the film are functions of wavelength and an iterative process involving interpolation is necessary to extract their values (Heavens, 2001).The complex refractive index, the frequency or wavelength are dependent on  $\mathbf{n}$  and  $\mathbf{K}$  via the so-called dispersion relations, the question is how  $\mathbf{n}$  and  $\mathbf{K}$  are interrelated and how  $\mathbf{n}$  and  $\mathbf{K}$  can be determined? Obviously this can be done by studying the transmission as a function of wavelength through a thin film of the material. There are available a number of experimental

techniques for measuring  $n$  and  $K$ . For example, ellipsometry measures changes in the polarization of light incident on a sample to sensitively characterize surfaces and thin films. The interaction of incident polarized light with the sample causes a polarization change in the light, which may then be measured by analyzing the light reflected from the sample.

## **2.5 Applications of thin films:**

The study of thin film phenomena dates back well over a century, it is really only over the last four decades that they have been used to a significant extent in practical situations. The requirement of micro miniaturization made the use of thin and thick films virtually imperative. The development of computer technology led to a requirement for very high density storage techniques and it is this which has stimulated most of the research on the magnetic properties of thin films. Many thin film devices have been developed which have found themselves looking for an application. In general these devices have resulted from research into the physical properties of thin films. Thin film materials have already been used in semiconductor devices, wireless communications, telecommunications, integrated circuits, rectifiers, transistors, solar cells, light-emitting diodes, photoconductors, light crystal displays, magneto-optic memories, audio and video systems, compact discs, electro-optic coatings, memories, multilayer capacitors, flat-panel displays, smart windows, computer chips, magneto optic discs, lithography, micro-electromechanical systems and multifunctional emerging coatings, as well as other emerging cutting technologies ( Rao and Shekhawat,2013).

## **2.6 Deposition techniques:**

There are a considerable number of processes that can be and are used for the deposition of optical coatings. The commonest take place under vacuum and can be classified as physical vapour deposition (sometimes abbreviated to PVD).In these

processes, the thin film condense directly in the solid phase from the vapour. The word ‘physical’ as distinct from ‘chemical’ is intended to indicate the absence of any chemical reactions in the formation of the film. This is an oversimplification. Chemical reactions are, in fact, involved but the term chemical vapour deposition (sometimes abbreviated to CVD) is reserved for a family of techniques where the growing film differs substantially in composition and properties from the components of the vapour phase (Macleod, 2001), (Yousif H. Alsheikh, 2018).

### **2.6.1 Chemical methods:**

Although physical vapour deposition is the predominant class of deposition processes in optical coatings, the application of chemical vapour deposition is gradually increasing. The chemical reactions between the starting materials, the precursors, to form the material of the coating may be triggered in various ways but the most common is probably by means of electrically induced plasma in the active vapour. Such processes are known collectively as plasma enhanced. Chemical vapour deposition is complementary to rather than a direct competitor of physical vapour deposition. It is especially useful in the deposition of organic polymer films that are largely beyond the capabilities of physical vapour deposition. The boundary between the two classes of process is rather blurred (Macleod, 2001). Because of the large category of chemical methods only a few of chemical methods are described here.

### **2.6.2 Physical methods:**

The physical vapour deposition processes can be classified in various ways but the most useful classifications for our purposes are based on the methods used for producing the vapour and on the energy that is involved in the deposition and growth of the films. Vacuum, or thermal, evaporation has for years been the principal physical vapour deposition process and because of its simplicity, its flexibility and its relatively low cost, and because of the enormous number of existing deposition systems, it is

likely to continue so for some considerable time. In thermal evaporation, the material to be deposited, the evaporant is simply heated to a temperature at which it vaporises. The vapour then condenses as a solid Film on the substrates, which are maintained at temperatures below the melting point of the evaporant. Molecules travel virtually in straight lines between source and substrate and the laws governing the thickness of deposit are similar to the laws that govern illumination. In sputtering, the vapour is produced by bombarding a target with energetic particles, mostly ions, so that the atoms and molecules of the target are ejected from it. Such vapour particles have much more energy than the products of thermal evaporation and this energy has considerable influence on the condensation and film-growth processes. In particular the films are usually much more compact and solid. In other variants of physical vapour deposition, the condensation of thermally evaporated material is supplied with additional energy by direct bombardment by energetic particles. Such processes, together with sputtering, are known collectively as the energetic processes (Macleod, 2001).

### **a- evaporation method:**

In thermal evaporation the vapour is produced simply by heating the material, known as the evaporant. Because of the reduced pressure in the chamber the vapour is given off in an even stream, the molecules appearing to travel in straight lines so that any variation in the thickness of the film that is formed is smooth, and depends principally on the position and orientation of the substrate with respect to the vapour source. The properties of the film are broadly similar to those of the bulk material, although, as we shall see, there are important differences in the detailed microstructure. Precautions that have to be taken to ensure good film quality include scrupulous cleanliness of the substrate surface, near normal incidence of the vapour stream and, sometimes, heating the substrate to temperatures of 200–300 °C (or even higher, depending on the material) before commencing deposition. The evaporation is carried out in a sealed

chamber that is evacuated to a pressure usually of the order of  $10^{-5}$  mb. The materials to be deposited are melted within the chamber, using one of a number of possible techniques that will be described. The complete plant consists of the chamber together with the necessary pumps, pressure gauges, power supplies for supplying the energy necessary to melt the evaporant, monitoring equipment for the measurement of the thin film thickness during the process, substrate holding jigs, substrate heaters and the controls (Macleod, 2001). The most common evaporation setup is shown in figure (2.5). Deposition techniques fall into two broad categories, depending on whether the process is primarily chemical or physical. Physical methods rely on evaporation or sputtering while chemical methods depend on specific chemical reaction.

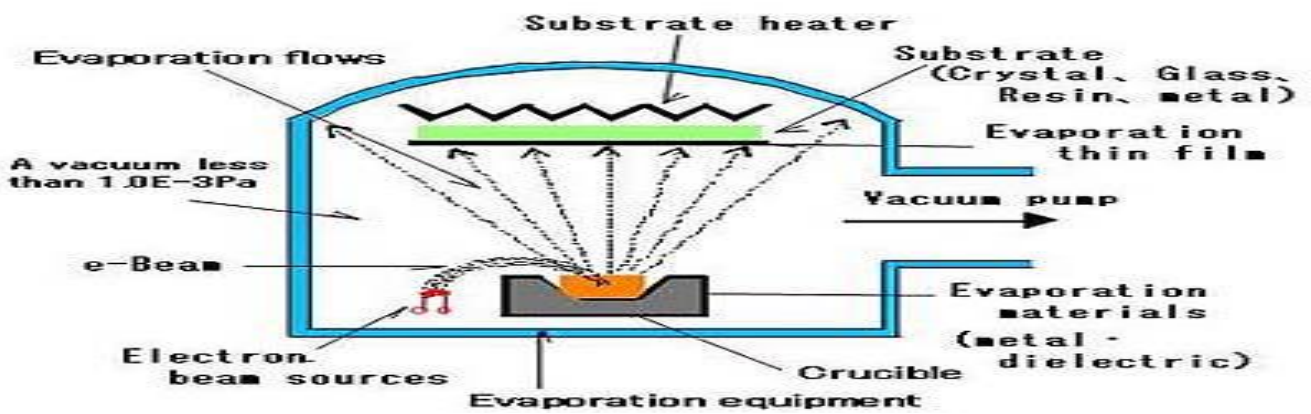


**Figure 2.5: Evaporation setup**

Figure (2.6) shows many useful processes for film deposition.

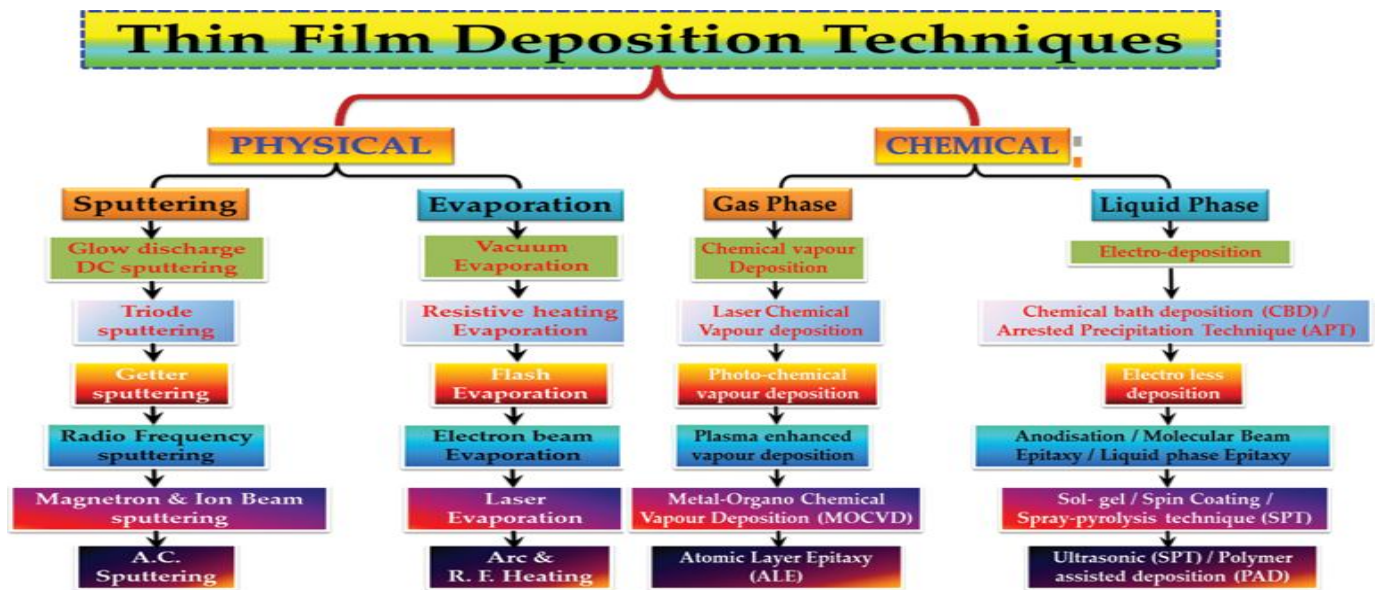


Figure 2.6: Most useful thin film deposition methods

### b- Sputtering method:

The electrode and gas-phase phenomena in various kinds of glow discharges (especially rf discharges) represent a rich source of processes used to deposit and etch thin films. Creative exploitation of these phenomena has resulted in the development of many useful processes for film deposition (as well as etching), as listed in figure 1.1. The most basic and well-known of these processes is sputtering, the ejection of surface atoms from an electrode surface by momentum transfer from bombarding ions to surface atoms. From this definition, sputtering is clearly an etching process, and is, in fact, used as such for surface cleaning and for pattern delineation. Since sputtering produces a vapor of electrode material, it is also (and more frequently) used as a method of film deposition similar to evaporative deposition. Sputter deposition has become a generic name for a variety of processes (Krishna Seshan, 2002).

#### 2.6.2 .1 Diode Sputtering

Diode sputtering uses a plate of the material to be deposited as the cathode (or rf-powered) electrode (target) in a glow discharge. Material can thus be transported from



the target to a substrate to form a film. Films of pure metals or alloys can be deposited when using noble gas discharges (typically Ar) with metal targets (Krishna Seshan, 2002).

#### **2.6.2.2 Reactive Sputtering**

Compounds can be synthesized by reactive sputtering, that is, sputtering elemental or alloy targets in reactive gases; alternatively, they can be deposited directly from compound targets.

#### **2.6.2.3. Bias Sputtering**

Bias sputtering, or ion-plating, is a variant of diode sputtering in which the substrates are ion bombarded during deposition and prior to film deposition to clean them. Ion bombardment during film deposition can produce one or more desirable effects, such as re-sputtering of loosely-bonded film material, low-energy ion implantation, desorption of gases, conformal coverage of contoured surface, or modification of a large number of film properties. The source material need not originate from a sputtering target, but can be an evaporation source, a reactive gas with condensable constituents, or a mixture of reactive gases with condensable constituents and other gases that react with the condensed constituents to form compounds. It should be noted that all glow discharge processes involve sputtering in one form or another, since it is impossible to sustain a glow discharge without an electrode at which these processes occur. In “electrodeless” discharges, rf power is capacitively coupled through the insulating wall of a tubular reactor. In this case, the inside wall of the tube is the main electrode of the discharge. However, sputtering can also lead to undesirable artifacts in this and other glow-discharge processes (Krishna Seshan, 2002).

#### **2.6.2.4. Magnetron Sputtering**

Another variant in sputtering sources uses magnetic fields transverse to the electric fields at sputtering-target surfaces. This class of processes is known as magnetron sputtering. Sputtering with a transverse magnetic field produces several important modifications of the basic processes. Target-generated secondary electrons do not bombard substrates because they are trapped in cycloidal trajectories near the target, and thus do not contribute to increased substrate temperature and radiation damage. This allows the use of substrates that are temperature-sensitive (for example, plastic materials) and surface-sensitive (for example, metal-oxides-semiconductor devices) with minimal adverse effects. In addition, this class of sputtering sources produces higher deposition rates than conventional sources and lends itself to economic, large-area industrial application. There are cylindrical, conical, and planar magnetron sources, all with particular advantages and disadvantages for specific applications. As with other forms of sputtering, magnetron sources can be used in a reactive sputtering mode. Alternatively, one can forego the low-temperature and low radiation-damage features and utilize magnetron sources as high-rate sources by operating them in a bias-sputtering mode ((Yousif H. Alsheikh, 2018).

### **2.6.2 .5. Ion-Beam Sputtering**

Ion beams, produced in and extracted from glow discharges in a differentially pumped system, are important to scientific investigations of sputtering, and are proving to be useful as practical film-deposition systems for special materials on relatively small substrate areas. There are several advantages of ion-beam sputtering deposition. The target and substrate are situated in a high-vacuum environment rather than in a high-pressure glow discharge. Glow discharge artifacts are thereby avoided, and higher-purity films usually result. Reactive sputtering and bias sputtering with a separate ion gun can be used (Krishna Seshan, 2002).

### **2.6.3 Pulsed laser deposition:**

In general, the method of PLD is simple. Only few parameters need to be controlled during the process. Targets used in PLD are small compared with other targets used in other sputtering techniques. It is quite easy to produce multi-layer film composed of two or more materials. Besides, by controlling the number of pulses, a fine control of film thickness can be achieved. Thus a fast response in exploiting new material system is a unique feature of PLD among other deposition methods. The most important feature of PLD is that the stoichiometry of the target can be retained in the deposited films. This is the result of an extremely high heating rate of the target surface ( $10^8\text{K/s}$ ) due to pulsed laser irradiation. It leads to the congruent evaporation of the target irrespective to the evaporating point of the constituent elements or compounds of the target. And because of the high heating rate of the ablated materials, laser deposition of crystalline film demands a much lower temperature than other mentioned film growth techniques. For this reason the semiconductor and the underlying integrated circuit can refrain from thermal degradation (Rao, 2013).

The technique of PLD has been used to deposit high quality films of materials for more than a decade. The technique uses high power laser pulses to melt, evaporate and ionize material from the surface of a target. This "ablation" event produces a transient, highly luminous plasma plume that expands rapidly away from the target surface. The ablated material is collected on an appropriately placed substrate upon which it condenses and the thin film grows. Applications of the PLD technique range from the production of superconducting and insulating circuit components to improved wear and biocompatibility for medical applications. In spite of this widespread usage, the fundamental processes occurring during the transfer of material from target to substrate are not fully understood and are consequently the focus of much research. In principle PLD is an extremely simple technique, uses pulses of laser energy to remove material from the surface of a target (Lackner, 2005).

### **2.6.3.1 Basics of PLD:**

The applicability and acceptance of pulsed laser deposition in thin-film research rests largely in its simplicity in implementation. Pulsed laser deposition is a physical vapor deposition process, carried out in a vacuum system, which shares some process characteristics common with molecular beam epitaxy and some with sputter deposition. In PLD, shown schematically in Figure 2.7, a pulsed laser is focused onto a target of the material to be deposited. For sufficiently high laser energy density, each laser pulse vaporizes or ablates a small amount of the material creating a plasma plume. The ablated material is ejected from the target in a highly forward-directed plume. The ablation plume provides the material flux for film growth. Historically Albert Einstein postulated the stimulated emission process in as early as 1916. The first optical master using a rod of ruby as the lasing medium was, however, constructed in 1960 by Theodore H. Maiman at Hughes Research Laboratories, a lapse of 44 years. Using laser to ablate material has to be traced back to 1962 when Breech and Cross used ruby laser to vaporize and excite atoms from a solid surface. Three years later, Smith and Turner used ruby laser to deposit thin films. This marked the very beginning of the development of the pulsed laser deposition technique. However, the development and investigations of pulsed laser deposition did not gather the expected momentum. In fact, the laser technology was immature at that time. The availability of the types of laser was limited; the stability output was poor and the laser repetition rate was too low for any realistic film growth processes. Thus the development of PLD in thin film fabrication was slow comparing with other techniques such as MBE, which can produce much better thin film quality. The rapid progress of the laser technology, however, enhanced the competitiveness of PLD in the following decade. The lasers having a higher repetition rate than the early ruby lasers made the thin film growth possible. Subsequently, reliable electronic Q-switches lasers became available for

generation of very short optical pulses. For this reason PLD can be used to achieve congruent evaporation of the target and to deposit stoichiometric thin films. The absorption depth is shallower for UV radiation. Subsequent development led to lasers with high efficient harmonic generator and excimer lasers delivering powerful UV radiation. From then on, non-thermal laser ablation of the target material became highly efficient. Pulsed laser deposition as a film growth technique has attained its reputed fame and has attracted wide spread interest after it has been used successfully to grow high-temperature  $T_c$  superconducting films in 1987. During the last decade, pulsed laser deposition has been employed to fabricate crystalline thin films with epitaxy quality. Ceramic oxide, nitride films, metallic multilayers, and various superlattices grown by PLD have been demonstrated. Recently, using PLD to synthesis nanotubes, nanopowders and quantum dots have also been reported. Production-related issues concerning reproducibility, large-area scale-up and multiple-level have begun to be addressed. It may start up another era of thin film fabrication in industry.

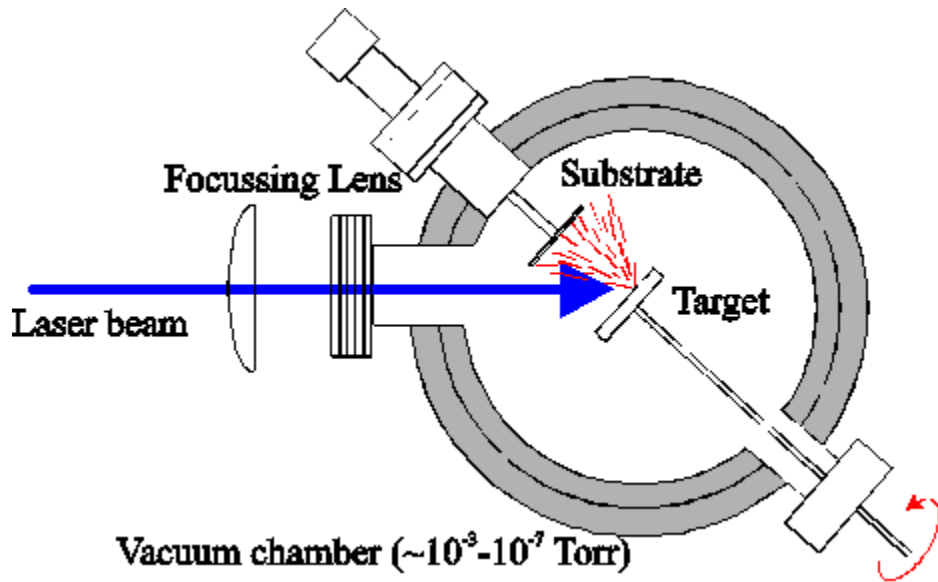


Figure 2.7: PLD setup

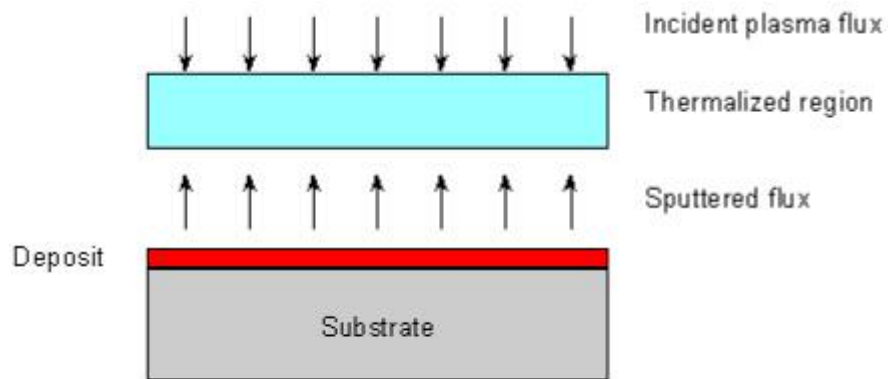
### 2.6.3.2 Mechanisms of PLD

The principle of pulsed laser deposition, in contrast to the simplicity of the system set-up, is a very complex physical phenomenon. It involves all the physical processes of laser-material interaction during the impact of the high-power pulsed radiation on a solid target. It also includes the formation of the plasma plume with high energetic species, the subsequent transfer of the ablated material through the plasma plume onto the heated substrate surface and the final film growth process. Thus PLD generally can be divided into the following four stages.

- Laser radiation interaction with the target
- Dynamic of the ablation materials
- Decomposition of the ablation materials onto the substrate
- Nucleation and growth of a thin film on the substrate surface

In the first stage, the laser beam is focused onto the surface of the target. At sufficiently high energy density and short pulse duration, all elements in the target surface are rapidly heated up to their evaporation temperature. Materials are dissociated from the target and ablated out with stoichiometry as in the target. The instantaneous ablation rate is highly dependent on the fluences of the laser irradiating on the target. The ablation mechanisms involve many complex physical phenomena such as collisional, thermal and electronic excitation, exfoliation and hydrodynamics. During the second stage the emitted materials tend to move towards the substrate according to the laws of gas-dynamic and show the forward peaking phenomenon R.K. Singh reported that the spatial thickness varied as a function of  $\cos^n \theta$ , where  $n \gg 1$ . The laser spot size and the plasma temperature have significant effects on the deposited film uniformity. The target-to-substrate distance is another parameter that governs the angular spread of the ablated materials. The third stage is important to determine the

quality of thin film. The ejected high-energy species impinge onto the substrate surface and may induce various type of damage to the substrate. The mechanism of the interaction is illustrated in the following figure. These energetic species sputter some of the surface atoms and a collision region is established between the incident flow and the sputtered atoms. Film grows immediately after this thermalized region (collision region) is formed. The region serves as a source for condensation of particles. When the condensation rate is higher than the rate of particles supplied by the sputtering, thermal equilibrium condition can be reached quickly and film grows on the substrate surface at the expense of the direct flow of the ablation particles. Figure (2.8) shows schematically the plasma-substrate interaction process.



**Schematic diagram of plasma-substrate interaction**

**Figure 2.8: plasma- substrate interaction**

Nucleation-and-growth of crystalline films depends on many factors such as the density, energy, degree of ionization, and the type of the condensing material, as well as the temperature and the physical-chemical properties of the substrate. The two main thermodynamic parameters for the growth mechanism are the substrate temperature  $T$  and the supersaturation  $\Delta m$ . They can be related by the following equation:

$$\Delta m = kT \ln(R / R_e) \quad (2-1)$$

where  $k$  is the Boltzmann constant,  $R$  is the actual deposition rate, and  $R_e$  is the equilibrium value at temperature  $T$ .

The nucleation process depends on the interfacial energies between the three phases present – substrate, the condensing material and the vapour. The minimum-energy shape of a nucleus is like a cap. The critical size of the nucleus depends on the driving force, i.e. the deposition rate and the substrate temperature. For the large nuclei, a characteristic of small supersaturation, they create isolate patches (islands) of the film on the substrates, which subsequently grow and coalesce together. As the supersaturation increases, the critical nucleus shrinks until its height reaches an atomic diameter and its shape is that of a two-dimensional layer. For large supersaturation, the layer-by-layer nucleation will happen for incompletely wetted foreign substrates. The crystalline film growth depends on the surface mobility of the adatom (vapour atoms). Normally, the adatom will diffuse through several atomic distances before sticking to a stable position within the newly formed film. The surface temperature of the substrate determines the adatom's surface diffusion ability. High temperature favours rapid and defect free crystal growth, whereas low temperature or large supersaturation crystal growth may be overwhelmed by energetic particle impingement, resulting in disordered or even amorphous structures.

### **2.6.3.3 Advantages of PLD:**

The advantages are counts for PLD over well-established physical methods of thin film deposition:



- PLD can work with almost any kind of material including non-volatile materials whereas molecular Beam epitaxy limits its choices with easily volatile materials only.
- Energy source (LASER) is placed outside the vacuum chamber which offers flexibility in geometrical arrangement of deposition system components as well as measurement systems if any.
- Due to local heating, material can be selectively deposited from a layered target also.
- Pulsed nature offer unique controllability of deposition thickness.
- High kinetic energy of plasma plume promotes surface mobility and hence high-quality crystalline films can be achieved in a relatively simpler way. At the same time, they can be tuned to avoid bulk displacements.
- Source material choice is virtually unlimited as choice of LASER parameters (like wavelength, intensity etc.) will determine the ablation process.
- Under suitable conditions, ratio of elemental components can be maintained exactly the same as the target material. This offers a great advantage as compared to other methods where many parameters need to be finely optimized and even finely maintained during the whole course of deposition.
- Ability to work in non-equilibrium conditions enables us to produce species with electronic states far from chemical equilibrium and hence novel and meta material's fabrication is much easier using PLD.
- The LASER-target interaction responsible for ablation process is completely decoupled from other process parameters like background gas, type of substrate

and substrate temperature. This results in better control of ablation dynamics for a variety of materials (Sandeep Nagar, 2012).

#### **2.6.3.4 Disadvantages of pulsed laser deposition:**

There are also disadvantages to perform PLD. Some of them are of a technical nature; some are intrinsic to the ablation process and the electromagnetic interaction between photons and matter:

- Light elements like oxygen or lithium have different expansion velocities and angular distributions in a plume as compared to heavier elements. Therefore, an addition source to supplement these elements to obtain the desired film composition is required, e.g., adequate background gas or an adapted target composition.
- Due to the high laser energies involved, macroscopic and microscopic particles from the target can be ejected which can be detrimental to the desired properties of films and multilayers. This can partially be overcome by working with very dense polycrystalline or even single crystalline targets, but it also depends on the absorption and mechanical properties of the target material and laser fluence used (Schneider, C. W., and Thomas Lippert, 2010).

The most addresses disadvantages for Pulsed laser deposition are:

- Formation of droplets poses a big disadvantage. Impurity of target materials will be reflected in thin films too. Hence great deal of care is necessary to avoid any impurity from the starting of experiments.

- Impurity in atmosphere of vacuum chamber will also be forced into thin film and hence high purity gases should be used and deposition chamber should be regularly cleaned after some set of depositions (particularly when targets are exchanged for depositions).
- Crystallographic defects are generated in the thin film due to impinging high kinetic energy species. This can be avoided by fine tuning the LASER energy and deposition pressure.
- Any inhomogeneity in flux and angular distribution of ablation plume is reflected as inhomogeneous thin film property. This can be avoided by polishing the target surface before mounting it on the target holder using suitable electronics to avoid instabilities fed to LASER.
- PLD depositions are limited to smaller areas usually few mm<sup>2</sup>. This can be improved by rotating the substrate holder and/or using multiple LASER beams.
- PLD is a batch process and cannot be used for continuous deposition of films. This is a major disadvantage from an industrial use point of view (Sandeep Nagar, 2012).

The presence of various types of particulates on the surface of the thin films deposited by pulsed laser deposition (PLD) is a strong limitation in key technological applications of this method. The presence of various types of particulates both on the surface of the films as well as in their bulk is a disadvantage. These micrometer and sub-micrometer sized particulates can be droplets, expelled in liquid phase from the target surface, or irregular shaped solid target material fragments. They represent the most important shortcoming for the application of the synthesized thin films in

technological fields, since in high performance electronic, optical and optoelectronic devices particulates-free films are required (E. Gyorgy, 2002).

In the description of the laser–plasma interaction, the laser pulse duration plays a crucial role: whereas in the case of nanosecond (ns) laser pulse, the forming plasma interacts with the laser beam” tail”, in the case of femtosecond (fs) laser pulse the previous mechanism doesn’t take place.

The laser absorption of the forming plasma reduces the efficiency of the energy deposition into the sample (plasma shielding effect) and increases the plume ionization degree, complicating the plume expansion mechanism (Alessia Sambri, 2008). Due to the plasma-laser interaction, the temperatures of the evaporated material increase therefore rapidly to extremely high values and the electrons are further accelerated. The excited particles will emit photons, leading to a bright plasma plume, which is characteristic for the laser ablation process (Blank, D.H.A., et al., 1992). The main absorption processes are the inverse Bremsstrahlung (IB) and the photoionization (PI), since the cross section of the other processes are much smaller ( Yousif H. Alsheikh, 2018); (Alessia Sambri, 2008).

## **2.7 Laser ablation and plasma formation:**

Laser ablation is a well-established method of removing material from a solid surface by irradiating it with a laser beam (T. MOŚCICKI et al., 2011).

Laser ablation is very complex, involving many simultaneous processes during and following the laser pulse such as heat transfer, electron-lattice energy exchange, material melting and evaporation, plasma plume formation and expansion, laser energy absorption etc. Pulsed laser ablation (PLA) has numerous applications making it an attractive area of fundamental research (Hussein A. E. et al., 2013). Applications includes laser machining (drilling, engraving), cleaning contaminated surfaces (removal of paint or coating), deposition of thin coatings on different materials,

production of new nanomaterials such as carbon nanotubes, laser-induced breakdown spectroscopy (LIBS), laser-ablation inductively coupled plasma mass spectrometry (LA-ICP-MS), elemental sensors (Hussein A. E. et al., 2013). In laser ablation, also called pulsed laser deposition (PLD), an intense, pulsed laser beam irradiates the target. When the laser pulse is absorbed by the target, its energy is used first for electronic excitation and converted into thermal, chemical, and mechanical forms of energy, resulting in evaporation, ablation, plasma formation, and even exfoliation. The ejected material expands into the surrounding vacuum in the form of a plume containing many energetic species, including atoms, molecules, electrons, ions, clusters, particles, and molten globules. These diverse species finally condense onto a substrate as a thin film (Martin, R. J., and Palma A.L., 2013).

During laser ablation, the material evaporated from the target forms a thin layer of very dense plume, this plasma plume absorbs energy from the laser beam (by means of photoionization and inverse Bremsstrahlung) and its temperature and pressure grow. The resulting pressure gradient accelerates the plume to high velocity perpendicular to the target (T. MOŚCICKI et al., 2011).

### **2.7.1 Expansion of the plasma plume in vacuum:**

In case of vacuum the plume, angular distribution is determined by the collisions of the plume particles among themselves in the initial stage. When plume is small however in the presence of the ambient gas the plume angular distribution is modified due to collision between the plume species and background gas atoms (Yahya, K.Z., 2010).

### **2.7.2 Expansion of the plasma plume into background gas:**

In the case of expansion into an ambient atmosphere, the plume acts as a piston compressing the background gas during its expansion. As a consequence of this

interaction, plume expansion along the direction normal to the target surface is broken to some extent, and the plume shape tends to be more and more hemispherical. For the sake of simplification, the theoretical analysis of plume propagation into an ambient gas is usually modeled for the case of a hemispherical plume.

## **2.8 Lasers for infrared laser ablation and deposition:**

The recent studies by Luther-Davies and collaborators on laser processing of materials using Ultrashort pulses at high pulse repetition frequency (PRF) represent a watershed in thinking about laser materials processing. Their approach is based on the idea that laser ablation thin-film deposition is best accomplished by a vaporization mechanism that employs relatively modest pulse energies to ablate a small amount of material, relatively high intensity to enhance cross section, and high PRF to optimize throughput. The first of these criteria ensures that collateral damage, particulate emission, and undue thermal loading are minimized. The second of these follows from the fact that reaction rates are fundamentally proportional to intensities and cross sections, rather than to fluence; in addition, at high intensities, nonlinear effects may produce additional yield of desirable products. High PRF serves both to maximize throughput and to produce a nearly continuous vapor stream during deposition. Up to now there have been few systematic tests of this novel materials-processing paradigm. Mode-locked Nd : YAG lasers have 100-ps pulses during which the material reaches thermal equilibrium and cannot deliver really high intensities, although good-quality films of amorphous carbon have been made in this way. Moreover, given their fixed frequencies, it is not possible to optimize the spatio-temporal density of electronic excitation in the ablation target (Robert Eason, 2007).

## **2.9 Deposition parameters:**

Target-substrate distance, partial pressure of oxygen, substrate temperature, laser pulse energy density and pulse repetition rate are the main five parameters that need to be optimized to get the desired films. It is important to recognize that highly stoichiometric, nearly single crystal-like epitaxial film is aimed for in the PLD method. Streams of ions or neutral atoms arrive at the surface of the substrate. The substrate surface consisting of positive and negative ions attracts ions of opposite charge thus initiating the layer growth. Layer by layer growth of crystal starts with the mobility of ions on the surface aided by their own kinetic energy and the substrate temperature. The process can be compared with the growth of ionic crystals from its solution on a seed crystal. Preferred growth rate is of the order of 1 Å per pulse (M S HEGDE, 2001); (Yousif H. Alsheik, 2018).

## **2.10 Literature Review:**

**C. R. IORDĂNESCU et al** in 2017 present work we study the optical, structural and morphological properties of CdS-doped glass films, deposited by Pulsed Laser Deposition (PLD) method. The glass target used for ablation was prepared by conventional melt-quenching technique and the semiconductor dopant, CdS powder, was embedded in the borosilicate melt glass host by continuous stirring. In order to improve the properties of the films, the laser wavelength was modified. Photoluminescence emission (PL) of CdS-doped glass films revealed a broad band located in the visible range. The structural analysis was carried out by micro-Raman spectroscopy, pointing out specific vibration modes for Si-O-Si bonds as well as for CdS dopant. The morphology and the chemical characterization of the films were investigated by Scanning Electron Microscopy (SEM), Energy Dispersive X-ray spectroscopy (EDX) and Atomic Force Microscopy (AFM).

**Eman M. Nasir 2014** A thin films of ZnS and ZnS: Al with various Al concentration (0, 1, 2)%wt has been prepared successfully. Also n-ZnS/p-Si and n-ZnS: Al/p-Si heterojunction detector (HJs) has been fabricated by thermal evaporation at different Al concentration. Structure of these films was characterized by X-ray diffraction. The structures of these films are cubic zinc along (111) plane. The reverse bias capacitance was measured as a function of bias voltage, and it is indicated that these HJs are abrupt. The capacitance decreases with increasing the reverse bias, and fixed at high value of reverse bias voltage. The capacitance increases with increasing Al concentration. The width of depletion layers decreases with increases Al concentration. The value of highest built in potential varies between (2-1.37V). The current-voltage characteristic of n-ZnS/p-Si and n-ZnS: Al/p-Si heterojunction show that the forward current at dark condition varies approximately exponentially with applied voltage and the junction was coincide with recombination-tunneling model, and reverse current exhibited a soft breakdown. The difference between forward and reverse current with applied voltage indicates that the detector has a high rectification characteristic. The value of ideality factor was varies between 2.58-3.22, and the value of tunneling constant ( $A_t$ ) varies between 4.92-8.05V<sup>-1</sup>. From the I-V measurements under illumination, the photocurrent increased with increasing Al concentration. The energy band diagram for HJ has been constructed.

**Balakrishnan G et al.,** in (2017) produced nanostructured single layer aluminium oxide ( $Al_2O_3$ ), single layer zirconium oxide ( $ZrO_2$ ) and the ( $Al_2O_3/ZrO_2$ ) nano multilayer films on Si (100) substrates at an optimized oxygen pressure of  $3 \times 10^{-2}$  mbar at room temperature by pulsed laser deposition. The  $Al_2O_3$  layer was kept constant at 5 nm, while  $ZrO_2$  layer thickness was varied from 5 nm to 20 nm. The X-ray diffraction (XRD) studies of single layer of  $Al_2O_3$  film indicated the cubic  $\gamma$ - $Al_2O_3$ , while the single layer of  $ZrO_2$  indicated both the monoclinic and tetragonal phases.



**E. M. NASIR and M. M. ABASS** (2016) have been prepared nanocrystalline thin films of PbS with different thickness (400,600) nm successfully by chemical bath deposition technique on glass and Si substrates. The structure and morphology of these films were studied by X-ray diffraction and atomic force microscope. It shows that the structure is polycrystalline and the average crystallite size has been measured. The electrical properties of these films have been studied, it was observed that D.C conductivity at room temperature increases with the increase of thickness, From Hall measurements the conductivity for all samples of PbS films is p-type. Carrier's concentration, mobility and drift velocity increases with increasing of thickness. Also p-PbS/n-Si heterojunction has been fabricated at different thickness. The reverse bias capacitance was measured as a function of bias voltage, and it is indicated that these HJs are abrupt. The capacitance decreases with increasing the reverse bias, and fixed at high value of reverse bias voltage. The capacitance increases with increasing thickness. The width of depletion layers decreases with increases thickness. The value of highest built in potential has been measured. The current-voltage characteristic show that the forward current at dark condition varies exponentially with applied voltage and the junction was coinciding with recombination-tunneling model. The difference between forward and reverse current with applied voltage indicates that the junction has a high rectification characteristic. The value of ideality factor was varies between (1.821-1.715), From the I-V measurements under illumination, the photocurrent increased with increasing thickness.

**Hamed M. A.** in (2015) was used pulsed laser deposition technique to produce silicon dioxide (SiO<sub>2</sub>) thin films on glass substrates at room temperature. The optical gap and linear refractive index of the prepared films were determined and their structures were found to be amorphous. Optical parameters were determined from UV-Visible absorption spectra in the spectral range of 200-850nm. The thickness of SiO<sub>2</sub> thin films

was measured by using an optical interferometer method employing He -Ne laser of 632nm wavelength at incident angle of 45°. The XRD pattern for films deposited at room temperature showed that the grown films are of amorphous structure. The effect of laser pulse energy on the optical properties has been studied. It was found that the optical properties reasonably depend on the laser pulse energy. The optical constants were determined from transmission and absorption spectra within the range of 200-800 nm for the deposited SiO<sub>2</sub> thin films. The refractive index as a function of the wavelength at different laser pulse energies was plotted and it was shown that the refractive index is almost constant in the range 400-600nm, and increases with increasing laser pulse energy. Also it was shown that from the variation relation of  $(\alpha h\nu)^2$  as a function of photon energy  $(h\nu)$  for SiO<sub>2</sub> deposited thin films energy gap is ranging from 1.7 to 3 eV depending on the laser pulse energy, as the energy band gap increases with increasing laser pulse energy.

**E. Marquez** in (2014) deposited various thicknesses of cadmium sulfide ZnS thin films were evaporated onto glass substrates using the thermal evaporation technique. X-ray diffraction analysis indicates that both the film and powder have cubic zincblende structure. The microstructure parameters, crystallite size and micro strain were calculated. It was observed that the crystallite size increases but the micro strain decreases with increase the film thickness. The band gaps of the ZnS thin films were found to be direct allowed transitions and increase from 3.33 to 3.46eV with increasing the film thickness. The refractive indices have been evaluated in transparent region using the envelope method in the transparent region. The refractive index can be interpolated and extrapolated in terms of Cauchy dispersion relationship over the whole spectra range, which extended from 300 to 2500nm. It was observed that the refractive index,  $n$  increase on increasing the film thickness.

**Bushra A. Hasan and Eman M. Nasir** in (2015) used thermal evaporation technique tin Sulphide (SnS) thin films have been deposited on glass slides have been deposited at room temperature using SnS powder. The deposited films have been investigated through X-ray diffraction measurements to determine structural properties. The deposited SnS films found polycrystalline with an orthorhombic structure. The grain size found to increase with thickness. The surface morphology of the films has been examined using atomic force microscopy AFM. The chemical compositions of the films have been determined using energy dispersive analysis of x-rays (EDAX). The dielectric properties of SnS thin films deposited with different thickness (100,200,and 300nm) are presented in this work. The dielectric permittivity  $\epsilon$  and ac conductivity  $\sigma_{ac}$  were measured at temperatures in the range of 293–493 K and frequencies in the range of 10 kHz–100MHz. It is found that there are two conductivity mechanisms and hence two activation energies converts to one mechanism with the increase of thickness. The ac activation energy EAC decreases with increase of thickness and frequency. The exponent  $s$  shows a progressive decrease with thickness. The results are explained in terms of structural difference by the effect of thickness and thermal treatment. Few anomalies in dielectric studies were observed near 340 and 440K, respectively. These points were related to crystalline phase transitions. Dark-conductivity and photo-conductivity increases with increase of thickness.

**De Mesa Joseph A. et al.,** in (2016) has successfully deposited undoped Zinc oxide on S(100) substrate by femtosecond pulsed laser. A mode-locked femtosecond laser operating at 790 nm wavelength, 100 fs pulse duration and 80 MHz repetition rate was used as an excitation source. The depositions were carried out at vacuum pressures of  $10^{-2}$ - $10^{-6}$  mbar and oxygen background gas pressures of  $10^{-2}$ - $10^{-4}$  mbar. Energy dispersive spectroscopy of samples grown without oxygen background gas shows higher zinc composition on deposited material as compared to oxygen that leads to off

stoichiometric ZnO films. Scanning electron microscopy (SEM) images shows that increasing oxygen gas pressure increased the particle size of the deposited ZnO. The material deposited at  $2 \times 10^{-4}$  mbar oxygen pressure revealed clustering of nanorods forming a flower-like structure that has an average length of 2700 nm and an average diameter of 450 nm. The X-ray diffraction spectra show c-axis orientation of the deposited ZnO with (002) and (110) reflection.

**F. A. La Porta** et al., in (2014) were prepared ZnS nanoparticles by a microwave-assisted solvothermal method, and the phase structure and optical properties along with the growth process of ZnS nanoparticles were studied. They report XRD, FE-SEM, EDXS, UV-vis and PL measurements, and first-principles calculations based on TDDFT methods in order to investigate the structural and electronic properties and the growth mechanism of ZnS nanostructures. The effects as well as the merits of microwave heating on the process and characteristics of the obtained ZnS nanostructures and their performance are reported.

**A.Z. Mohammed** et al., in (2018) were prepared and investigated the effects of the number of shots of laser and annealing temperature on the structural, morphological, and optical properties of zinc sulfide nanoparticles (ZnS NPs) thin films by pulsed laser deposition technique (PLD), titled. XRD results show that ZnS NPs exhibit a hexagonal phase at 623K. Transformation in the shape of nanoparticles to nanoflowers and nanorods appeared with increasing number of shots of laser at the same annealing temperature (623K) was observed from scanning electron microscopy (SEM) images. The optical properties were studied from all transmittance data. The experimental results show that the as-deposited ZnS NPs film exhibit a cubic structure and the crystallinity increased in the annealed films. It is also found that the grain size of the as grown samples at 300 K, rises linearly from 9 to 11 nm with increasing the number of shots from 1000 to 3000 and rapidly from 10 to 18 nm after annealing at 623K.

Additionally, the increase of the number of shots from 1000 to 3000 leads to a decrease in the energy gap values and increases their values after heat treatment keeping their behavior decreasing as the number of shots of laser increases. Also, photoluminescence (PL) measurements explained quenching its value after annealing temperature.

**Eman M.N.Al-Fawadi et al.**, in (2008) Fabricated a polycrystalline CdSe thin films doped with (5 wt %) of Cu using vacuum evaporation technique in the substrate temperature range ( $T_s=R_T-250$ ) °C on glass substrates of the thickness (0.8 $\mu$ m). The structure of these films are determined by X-ray diffraction (XRD).The X-ray diffraction studies shows that the structure is polycrystalline with hexagonal structure, and there are strong peaks at the direction (200)at ( $T_s=R_T-150$ )°C, while at higher substrate temperature( $T_s=150-250$ )°C the structure is single crystal. The optical properties as a function of  $T_s$  were studied. The absorption, transmission, and reflection has been studied, the optical energy gap ( $E_g$ ) increases with increase of substrate temperature from (1.65-1.84) eV due to improvement in the structure. The amorphousity of the films decreases with increasing  $T_s$ . The films have direct energy gap and the absorption edge was shift slightly towards smaller wavelength for CdSe:Cu thin film with increase of substrate temperature. it was found that the absorption coefficient was decreased with increasing of substrate temperature due to increases the value of( $E_g$ ). The CdSe:Cu films showed absorption coefficient in the range (0.94x10<sup>4</sup>-0.42x10<sup>4</sup>) cm<sup>-1</sup>at  $T_s=R_T-250$ °C.Also the density of state decreases with increasing of substrate temperatures from (0.20-0.07)eV, it is possibly due to the recrystallization by the heating substrate temperatures. Also the extinction coefficient, refractive index and dielectric constant have been studied.

**M. A. Sangamesha et al.**, in (2013) developed a dye-sensitized nanocrystalline copper sulphide (CuS in thin film structure) solar cell using crystal violet (CV) as a photosensitizer us. Nanocrystalline CuS thin film is deposited on indium tin oxide-

(ITO-) coated glass substrate by chemical bath deposition (CBD) technique. These thin films are characterized for their structural, optical and electrical properties using X-ray diffractometer (XRD), atomic force microscopy (AFM), and scanning electron microscopy (SEM). Optical absorbance measurements from UV-visible spectrometer at normal incidence of light in the wavelength range of 320–1100 nm and current-voltage (I-V) measurements were also made. The deposited CuS thin film on ITO-coated glass substrate may be used as a photo electrode in the fabrication of dye-sensitized solar cell (DSSC). The carbon soot collected on the substrate is used as a counter electrode. The counter electrode coupled with a dye-sensitized CuS thin film along with a redox electrolyte mixture is used to develop a complete photovoltaic cell. The fill factor and efficiency were evaluated for the developed DSSC.

Zinc sulfide (ZnS) thin films were deposited by **Dr. Kadhim Abid Hubeatir** in (2015) on a glass and n-type Silicon wafer substrates at temperature range from 50 – 200 °C using pulsed laser deposition (PLD) technique. The structural, morphological, optical and electrical properties of the films have been investigated. The XRD analyses indicate that ZnS films have zinc blende structures with plane (111) preferential orientation, whereas the diffraction patterns sharpen with the increase in substrate temperatures. The Atomic Force Microscopy (AFM) Images shows the particle size and surface roughness of the deposited ZnS thin film at substrate temperature 50 and 150 °C were about 62.90 nm, 74.68nm respectively. Also we noticed that the surface roughness is increased at substrate temperature 150 °C compared with temperature 50 °C. At 200 °C the formed films exhibit a good optical property with 80% transmittance in the visible region. The electrical properties confirmed that they depend strongly on the bias voltage and the amount of current produced by a photovoltaic device which is directly related to the number of photons absorbed. C-V results demonstrated that the fabricated heterojunction is of abrupt type.

**J.J. Hassan** in (2006) prepared zinc sulfide by thermal evaporation technique on glass substrate, at different substrate temperatures. Film structure and grain size were determined by X- ray diffraction (XRD) device. Films have cubic polycrystalline structure with lattice constant  $a=5.41$  Angstrom, the optical constants (refractive index and absorption coefficients) of the films were derived from transmission spectra in the wavelengths range 300-700 nm. Data are analyzed by Swanepoel method increasing of substrate temperature, the refractive index of films was increased and all films have nearly same refractive index at wavelength about 630 nm. Optical band of prepared films are in the range 3.4-3.62 eV and was increased with increasing substrate temperature. The aim of his study was to obtain matched properties from ZnS thin films to be used in solar cell applications.

# CHAPTER THREE

## EXPERIMENTAL PART

### **3-1 Introduction:**

This chapter describes the details of the experimental part of this thesis, defining the materials used, their properties, the equipment to prepare them for deposition process (pressing the powder into disc form), the Q-switched Nd:YAG laser source used for the fabrication of the thin zinc sulphide films, also discuss the technique used to determine the thickness of the deposited films, the methodology followed to fabricate the zinc sulphide films; and the method of optical properties determination with the equipment and tools used were also presented in this chapter.

### **3-2 Materials used:**

The materials used in this work were zinc sulphide ZnS, of high purity and Potassium bromide- KBr (IR spectroscopy grade), they were in powder form mixed together and pressed to form solid disk target. The full information about the potassium bromide and Silicon oxides used in this work with their properties are described below:

#### **3-2-1 Potassium bromide (KBr):**

Potassium Bromide (KBr) is one of the most useful materials for general **purpose** spectroscopic windows and applications where sensitivity to moisture is unimportant. Potassium Bromide is the most commonly used beam splitter material for IR spectrophotometers. It can be supplied with a conformal polymer coating to give some protection against atmospheric humidity (Crystran ltd, 2018). Figure (3.1) shows the transmission spectrum of the KBr from 0.2 to 40 microns.



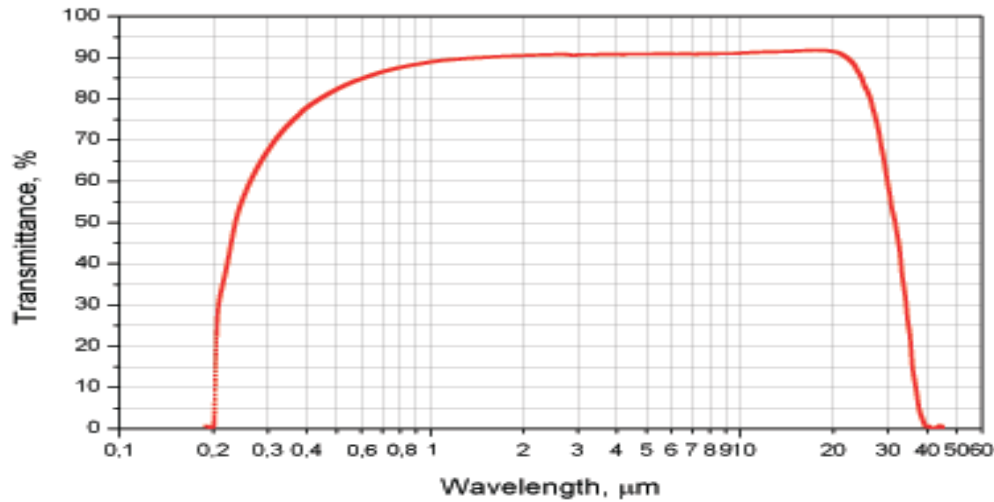


**Figure 3.1: transmission spectrum of the KBr**

### **3-2-2 Zinc Sulphide ZnS:**

ZnS is one of the first semiconductors discovered that has shown the remarkable properties that can be exploited for versatile applications including field emitters, electroluminescence, electro catalyst, biosensors. Compared to bulk ZnS, nano ZnS possess anomalous physical and chemical properties such as: enhanced surface to volume ratio, the quantum size effect, surface and volume effect and macroscopic quantum tunneling effect, more optical absorption, chemical activity and thermal resistance, catalysis, and the low melting point. Zinc Sulphide (ZnS) is a wide gap and direct transition semiconductor that belong to group II-VI semiconductors. ZnS thin films are believed to be one of the most promising materials for blue light emitting diodes, and in electroluminescent displays. As a result, ZnS is an important material used as an antireflection coating in heterojunction solar cells. And in Infrared windows, there are many challenges to produce this material in thin film structure. There exist several methods to produce thin films from this material such as sol-gel, rf-sputtering, pulse laser deposition, and so on. Zinc sulphide (ZnS), being an important II-VI group semiconductor with its excellent physical properties has recently been

investigated extensively due to its wide band gap and high refractive index. Furthermore, ZnS crystallizes into two allotropic forms: a cubic form (c-ZnS) with sphalerite structure having band gap of 3.5–3.7eV and a hexagonal form (h-ZnS) with wurtzite structure having band gap of 3.7–3.8 eV.

### 3-2-2-1 ZnS properties:

The most important properties of the Zinc sulphide is shown in table (3.1).

**Table 3.1: the most important properties of the ZnS:**

Chemical formula	ZnS
Molecular weight	97.46 g/mol
Group	Zinc-12
Sulphur-16	Sulphur-16
Crystal structure	Cubic
Lattice Constant 5.4093	5.4093
Dielectric Constant	8.9
Electronic configuration	Zinc [Ar] 3d <sup>10</sup> 4S <sup>2</sup>
	Sulphur [Ne] 3s <sup>2</sup> 3p <sup>4</sup>
Band Gap	3.54 eV
Electron Mobility	180 cm <sup>2</sup> /Vs
Hole Mobility	5 cm <sup>2</sup> /Vs
Refractive Index	1.46
Heat of Fusion	390 J/g
Heat of Formation	477 KJ/mol

Thermal coefficient of Expansion	6.36 $\mu\text{m/m C}$
Thermal Conductivity	25.1 W/mK
Specific heat capacity	0.472 J/g C

### 3-2-2-2 Applications of ZnS:

It has wide range applications including light-emitting diodes (LEDs), flat panel devices, solid state solar window layers, phosphors, photoconductors, catalysts, production of hydrogen, blue light diodes, electro-luminescent displays, antireflection coating for infrared devices and other non-linear optical devices. The most common structure of the ZnS found in nature is shown in figure (3-2).

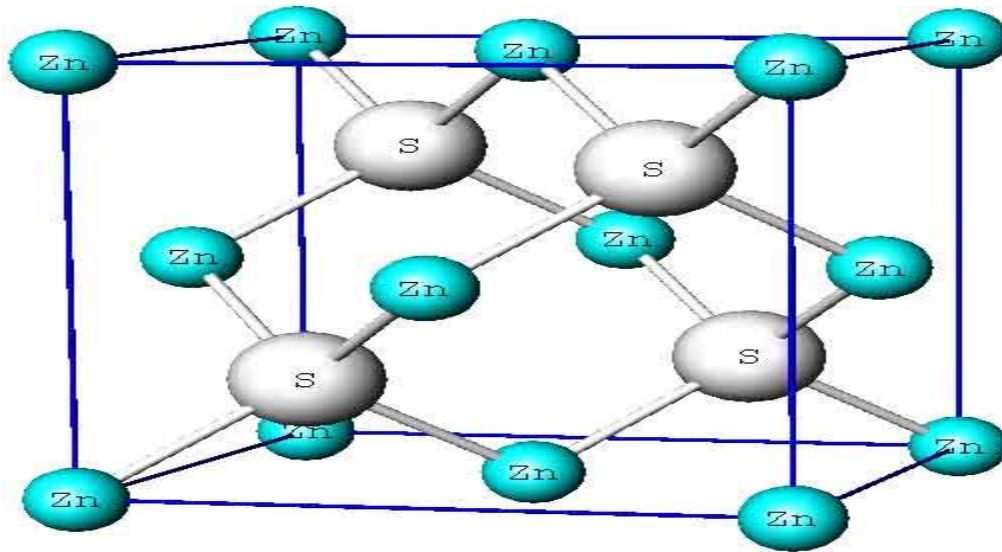


**Figure 3.2: The ZnS structure**

ZnS powders with high purity (95.5%) pressing it under 20 KN to form a target with 2.5 cm diameter and 0.4 cm thickness. The target should be as dense and homogenous as possible to ensure a good quality of the deposit.

### **3-3 Target preparation, machine and method:**

ZnS powder with high purity (95.5%) were mixed with the potassium bromide (IR spectroscopy grade) with 50: 50 ratios, pressing it under a pressure of 20 KN using a pressing machine hand press model SSP-10 A in Khartoum university the pressing machine imported from Shimadzu Kyoto- Japan .The Shimadzu pressing machine was used in order to produce solid rigid disks by pressing them in disk shape. The load provided by this machine extended from 0.0 to 15.0 tons. The part accompanied with this Machine is of an internal radius of about 15 mm and a height of about 100 mm. the base, the sides, the cover of this part are all very smooth. The target should be as dense and homogenous as possible to ensure a good quality of the deposit.

### **3-4 Substrates**

The substrates used to deposit the oxides thin films were glass with 1 mm thickness, and dimensions, 2X2 cm, and it's a refractive index of 1.5

### **3-5 The Q-Switched Nd: YAG laser source:**

Nd: YAG lasers are possibly the more widely used lasers either for basic research or for industrial and technological applications. These lasers are also excellent pump sources for laser development, for instance Ti: Sapphire ultrashort pulse lasers are based on CW Nd: YAG pumping. In particular, Nd-YAG lasers have been applied to study laser-induced oxidation in metals as titanium and chromium; semiconductors as silicon dioxides (Yousif Alsheikh, 2018). (Perez del Pino, A. et al., 2004) demonstrated that the rutile phase of  $\text{TiO}_2$  is obtained by laser oxidation in air of titanium films. Nd:YAG laser pulses have been used to laser-induce a phase transformation from  $\text{W}_3\text{O}$  thin films to  $\text{WO}_3$  (Evans R., et al., 2007); laser ablation for micromachining of bulk metals as copper, bronze and aluminum has also been done using Nd:YAG nanosecond pulses

(Yousif Alsheikh 2018), The Q- switched Nd: YAG laser is a solid state type laser emits 1064 nm as the fundamental wavelength, and it emits 532 nm wavelength using frequency doubling technique via nonlinear crystals such as KDP crystals, and its possible to get 1320 nm wavelength from the Q- switched Nd: YAG source using frequency. The Q-switched Nd: YAG laser source model OW-D1 used to fabricate the oxide thin films was imported from china it's used mainly for beauty and treatment purposes such as vascular therapy and hair removal, etc. (Oriental Wison Michanical & Electronics Co. Ltd., 2017).Figure (3.3) shows the user interface of Q-Nd: YAG laser source OW-D1 source.

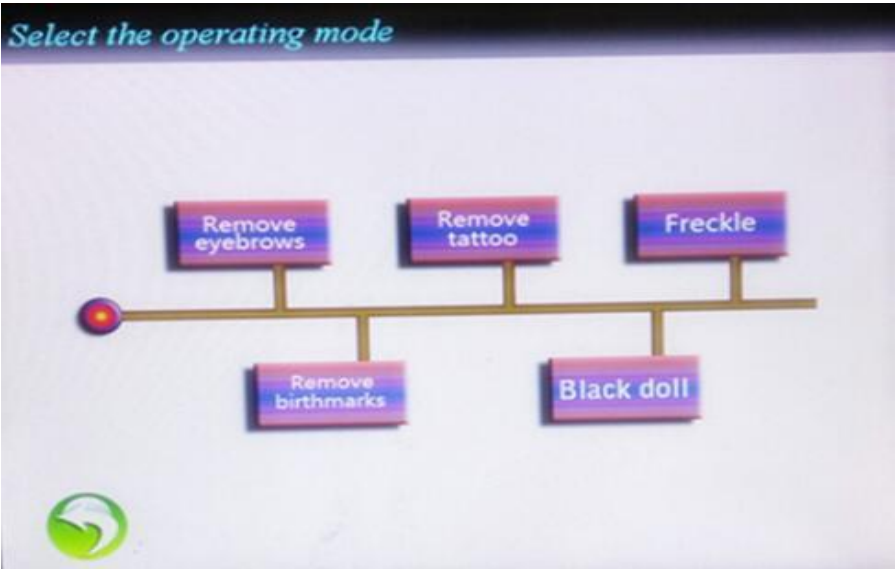


**Figure 3.3: User interface of Q-Switched Nd: YAG laser source model OW-D1**

**3-4-1 Q-switched Nd: YAG (OW-D1 model) specifications:**

The important features of the Q-switched Nd: YAG (OW-D1 model) are illustrated in table (3-2).

**Table 3.2: Specifications of the Q-switched Nd: YAG laser source:**

Product Name	ND YAG LASER Age spot removal machine (OW-D1)
Model No.	OW-D1
Type	Spot removal machine
Theory	Laser
Application	Clinic
Machine type	Laser Age Spot removal machine
Treatment head	1064nm/ 532 nm/ 1320 nm (Moppet Head)
Spot size	1-8 mm
Frequency	1-6 Hz
Energy	Up to 2000 mJ
Operating screen	5.7 Inches Key press screen
Indicator	Infrared ray indicator light
Input power	AC 220 V (110 V) / 15 A --- 50 Hz (60 Hz)
Pulse width	10 ns

### **3-4-2 Advantages:**

The machine has two important advantages, in addition to the multiple languages of the machine they are: **a-** Safe and efficient this is due to the automatic device of water –

level and water temperature make the use of the machine safe and efficient., **b-** portable and easy operation the OW-D1 device is a user friendly LCD touch-screen makes operation easy, its collimator make operation safe, accurate and efficient (Oriental Wison Mechanical & Electronics Co. Ltd., 2017).

### **3-5 Field Emission Scanning Electron microscopes:**

As all other kinds of scanning electron microscopy the field emission scanning electron microscope imaged the samples using the accelerated electrons. Accelerated electrons in an SEM carry significant amounts of kinetic energy. And those electrons go and interact with the sample. There are four possibilities of emission of x-rays, backscattered electrons, secondary electrons and auger electrons when the electron hit the sample. Detectors are used to collect them and convert into signal. The most common imaging mode collects low-energy (<50 eV) secondary electrons that are ejected from the k-orbitals of the specimen atoms by inelastic scattering interactions with beam electrons (Yousif Alsheikh, 2018). Field Emission Scanning Electron Microscope (FE-SEM) is one of the most powerful techniques for studying surface fine structures with resolution better than of SEM. New instrumental developments, such as an improved objective lens with lower aberrations coupled with an aberration corrector have been reported to improve the resolution of SEM images in a general sense (S. Asahina et al., 2012). FESEM is a powerful and popular technique for imaging the surfaces of almost any materials with a resolution down to about few nm. The image resolution offered by SEM depends not only on the property of the electron probe, but also on the interaction of the electron probe with the specimen. The interaction of an incident electron beam with the specimen produces secondary electrons, with energy typically smaller than 50 eV, the emission efficiency of which sensitively depends on surface geometry, surface chemical characteristics and bulk chemical composition. SEM can thus provide information about the surface topology, morphology and

chemical composition. FESEM gives clearer and less distorted pictures with spatial resolution to  $1\frac{1}{2}$  nm which is 3-6 times better than the conventional SEM. In addition to that it produces high quality and low voltages images with negligible electrical charging of samples (Panda, R.Kumar, 2015).

Schematic diagram of the scanning electron microscope is shown in figure (3.4).

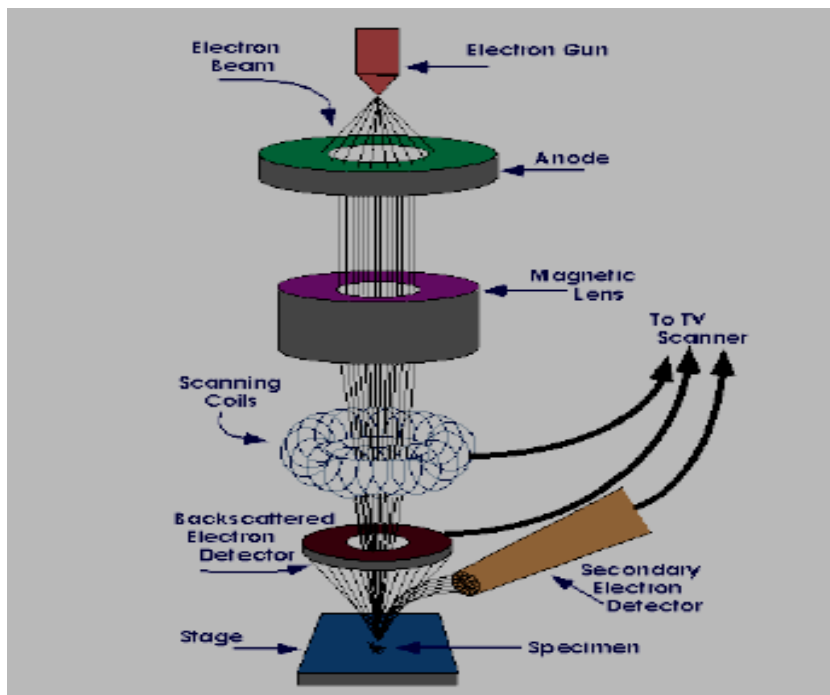


**Figure 3.4: Schematic diagram of the scanning electron microscope**

Field Emission-Scanning Electron Microscope type MIRA3 was used in this work was manufactured by Oxfords instruments.

MIRA3 is a high performance SEM system which features a high brightness Schottky emitter for achieving high resolution and low-noise imaging. MIRA3 offers all the advantages that come with the latest technologies and developments in SEM; delivering faster image acquisition, an ultra-fast scanning system, dynamic and static compensation and built-in scripting for user-defined applications. Its excellent



resolution at high beam currents has proven to be especially advantageous for EDX used for probing and analyzing the chemical constituents of the sample that imaged by the FESEM, WDX and EBSD compositional analyses. The capabilities for imaging at low landing electron energies are further enhanced by means of the optional beam deceleration technology (BDT).

A photograph of the MIRA3 FESEM used in this work was shown in figure 3.5 below:



**Figure 3.5: A photograph of the FESEM, shown**

### **3-5-1MIRA3 KEY FEATURE:**

The most important advantages of the FESEM type MIRA3 are:

1. High brightness Schottky emitter for high-resolution/high current/low-noise imaging.
2. Excellent imaging at short working distances with the powerful In-Beam detector (optional).
3. Investigation of non-conductive samples in variable pressure modes.

4. All MIRA3 chambers provide superior specimen handling using a 5-axis fully motorized computer centric stage and have ideal geometry for EDX and EBSD.
5. Optional extra-large chambers (XM, GM) with robust stages able to accommodate large samples including large wafers (6", 8", 12") are also available.
6. Several options for chamber suspension type ensure effective reduction of ambient vibrations in the laboratory.
7. Non-distorted EBSD pattern.

The most important part of the MIRA3 FESEM is the sample stage that contains the electron probe; the FESEM type MIRA3 comes with the stages that are capable of investigating seven different samples at the same time. But the sample stage require high attention when opened to put the sample/or samples under investigation a gloves should be wears to avoid accumulation of the carbon inside the stage which may results in bad image (Yousif Alsheikh,2018)

### **3-5-2 The FESEM MIRA3 stage and the sample holder:**

The sample holder and stage of the FESEM MIRA3 type is shown in figure (3.6) the figure illustrates samples under inspections.



**Figure 3.6: FESEM stage and sample holder**

### **3-6 Methodology of ZnS thin films deposition and characterization:**

The procedure to fabricate ZnS thin films and study the influence of the number of the laser pulses and to study the effect of pulse energy on their properties was done as follows: First of all, different disks of ZnS (as targets) were prepared by the press machine. And the experimental setup used to produce ZnS thin films was arranged as shown in figure (3.7)

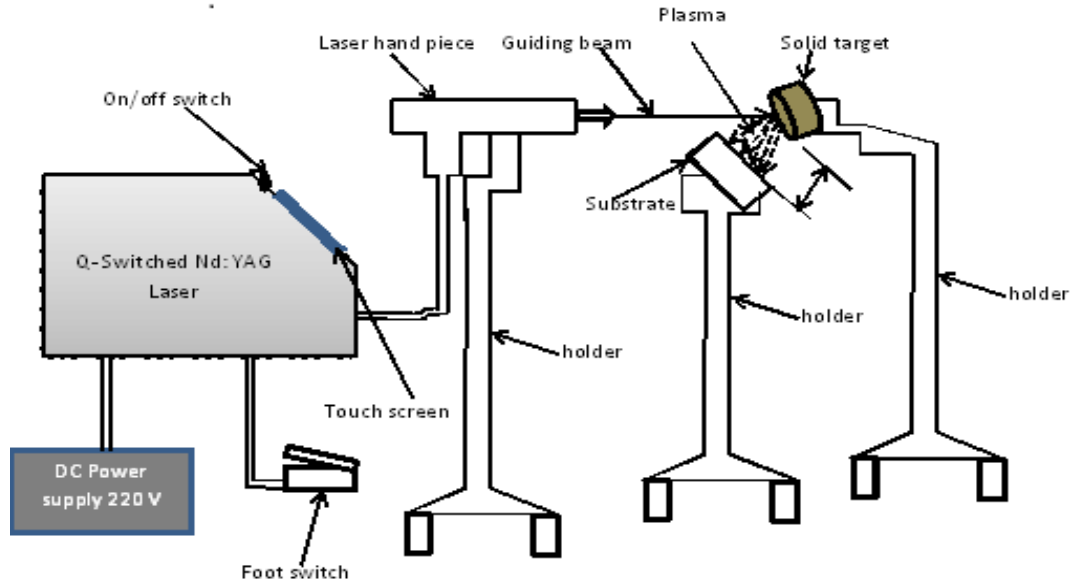


**Figure 3.7: The experimental setup for fabrication of ZnS thin films**

The distance and the angle between the target and the glass substrate were fixed to 2 cm, and  $45^\circ$ , respectively, the glass substrates were cut into the dimensions suitable for FESEM imaging 2X2 cm, and then washed with distilled water and cleaned with alcohol. After the arrangement as shown in figure (1), the Q-Switched Nd: YAG laser machine was switched on and 10 pulses with laser pulse energy of 100 mj and 2 Hz R.R was used to deposit ZnS thin film on the glass substrate. Then the produced thin film sample was carefully taken off and a new substrate is used and the previous step was repeated three times with varied number of (15, 20, and 25) of laser pulses with fixed repetition rate and pulse energy were used. Then the fabricated ZnS thin films were examined using FESEM to measure their thicknesses. The optical properties were measured by using the setup shown in figure (3.8).

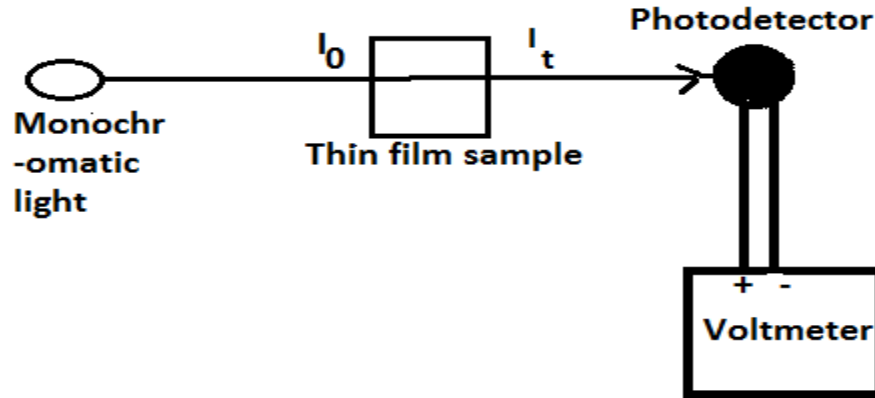


**Figure 3.8: Diagram of the experimental setup for optical measurement of ZnS thin films**

Each sample of the fabricated thin films was placed in aligned position with the monochromatic light sources whose wavelengths ranges from 532 nm to 915 shown in (table 3.3)

**Table 3.3: the laser sources used for transmission spectra measurement:**

Laser Source	Wavelength (nm)
Diode Laser	532
He-Ne Laser	632.8
Diode laser	660
Omega XP Laser (red probe)	675
Omega XP Laser (IR probe)	820
Omega XP Laser (IR probe)	915

The intensity of the monochromatic light sources were detected before (incident intensity  $I_0$ ) and after (transmitted intensity  $I_t$ ) the sample, the values of the transmitted and incident intensities of each sample were recorded for all monochromatic and were used to calculate the transmission percentage from  $T\% = I_t/I_0$ , and measured thicknesses of the fabricated thin films samples together with the

transmission data recorded were used to deduce the fabricated ZnS thin films optical properties as follows; First the refractive index of each thin film was calculated using the measured reflectivity **R** and the glass refractive index  $\mu$  according to (Hussein, M.T., et al., 2012); (Yousif H. Alsheikh, 2018) as:

$$\mu = \left( \frac{\mu_s [1 + \sqrt{R}]}{1 - \sqrt{R}} \right)^{\frac{1}{2}} \quad (3.1)$$

$$\mu_s = \frac{1}{T_s} \left( \frac{1}{T_s^2} - 1 \right)^{\frac{1}{2}}$$

Where,  $T_s$  represents the transmission of glass substrate.

Then the absorption coefficients of the ZnS fabricated thin films were deduced from the measured value of reflectivity **R**, transmittance **T**, refractive index  $\mu_s$ , and thickness **t** according to ( Almuslet and Alsheikh, 2015); (Hussein, M.T., et al., 2012) as:

$$\alpha = \frac{1}{t} \mu \frac{(1-R)^2}{T} \quad (3.2)$$

Then after the relation between the number of laser pulses and the ZnS thin film thickness was plotted and the transmission spectra of the fabricated ZnS films were recorded using different laser sources. Then the measured thicknesses of the ZnS films and the transmission data recorded were used to calculate the optical properties for each film. The same procedure was used in case of depositing the ZnS using different laser pulse energy of (125,150,175 and 200) mj with the same deposition conditions pulse repetition rate of 5 Hz, and the same laser wavelength of 1064 nm, the same target to substrate distance and angle of 2 cm, and 45° the characterization and measurement using the same devices and method.

# CHAPTER FOUR

## RESULTS AND DISCUSSION

### **4-1 Introduction:**

This chapter presents in details the results, discussion, conclusion and recommendations of these thesis.

### **4-2 Number of Pulses Influences thickness and optical properties of ZnS thin films:**

The results of the influence of the number of laser pulses on the thickness and optical properties of ZnS thin films fabricated using pulse laser deposition method is presented hereunder: In this case four samples of ZnS thin film were fabricated using Q-switched Nd: YAG pulsed laser deposition with the wavelength of 1064 nm, 100 mj pulse energy with pulse repetition rate of 2 Hz, the target to substrate distance and angle were fixed to 2 cm and 45°, respectively. Varied number of (10, 15, 20 and 25) of the laser pulses was used. The film thickness was measured by Field Emission scanning Electron Microscope (FESEM) measurement tool, and the transmission spectrum at certain wavelengths for each film was recorded. ZnS thin films transmission data and the measured film thicknesses were used to calculate their optical properties.

Figures (4.1,a) and (4.1,b) shows the FESEM image and the measurement of the thickness of the ZnS thin film deposited when the pulse energy was 100 mj, the pulse repetition rate is 2 Hz, and , the target to substrate distance and angle were fixed to 2 cm and 45°, respectively .

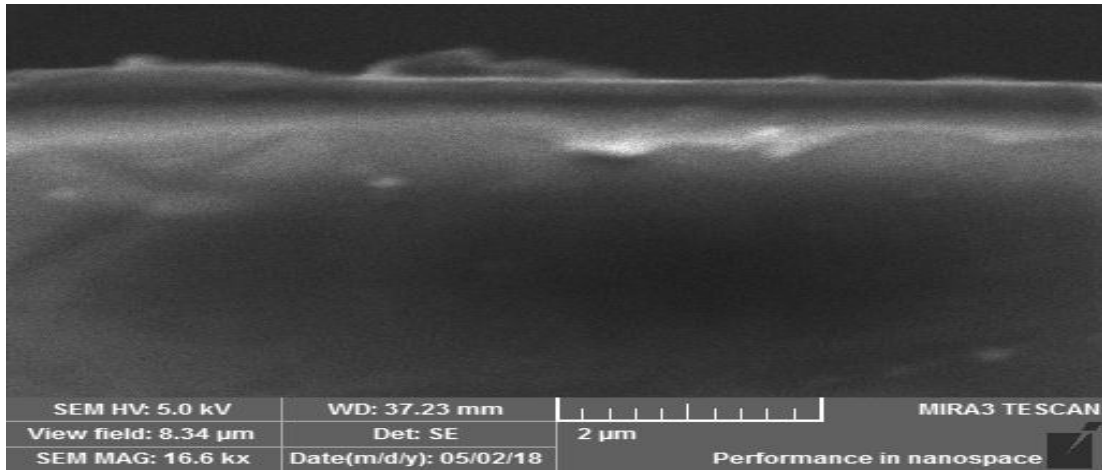


**Figure (4.1, a): FESEM image of ZnS thin film deposited on glass substrate with 10 laser pulses, laser pulse energy of 100 mj and repetition rate of 2 Hz**

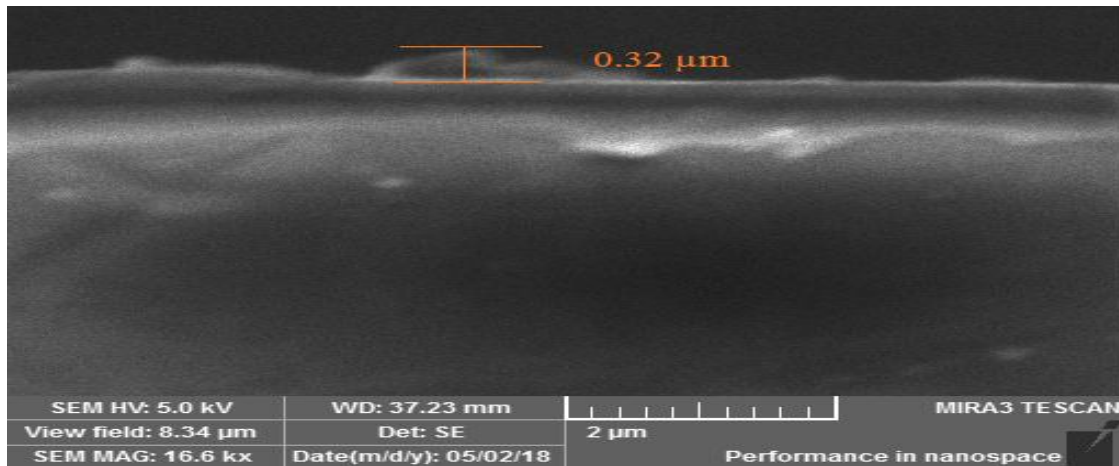
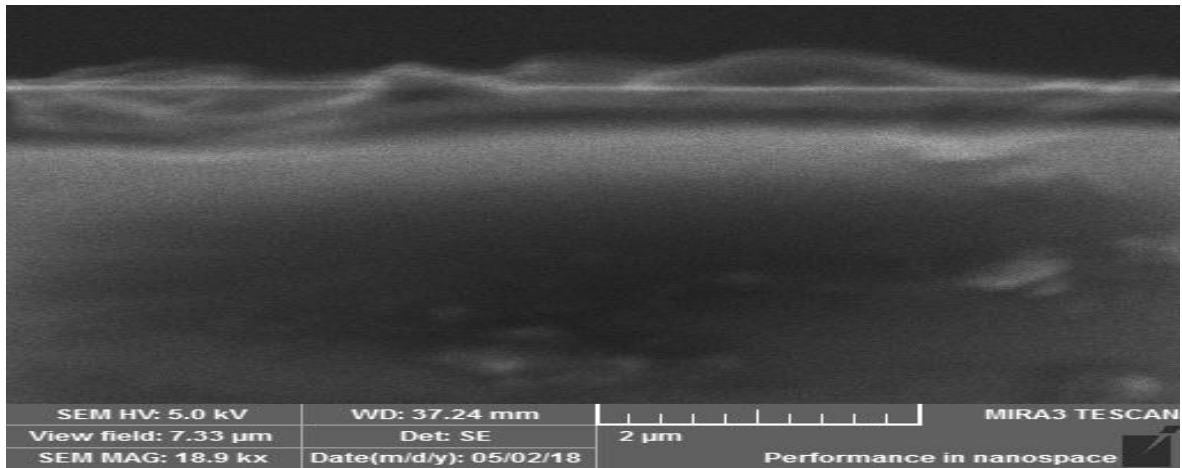


**Figure (4.1, b): FESEM image of thickness size measurement of ZnS thin film deposited on glass substrate with 10 laser pulses, laser pulse energy of 100 mj and repetition rate of 2 Hz**

The FESEM image together with the thickness measurement shown in figures (4.1 a, and b), respectively, illustrate that the ZnS thin film deposited has a thickness of 0.32  $\mu\text{m}$  and it's clear that the fabricated film is dense and has smooth film morphology.

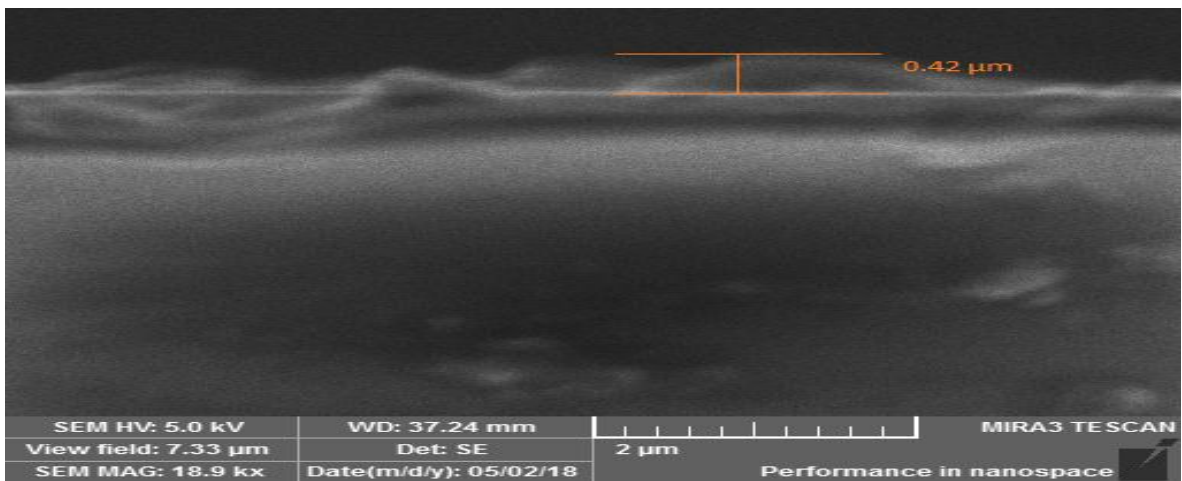
Figure (4.2, a) shows the FESEM image of the ZnS thin film sample fabricated when the pulse energy, the pulse repetition rate and the target to substrate distance and angle were fixed the only varied parameter was the number of laser pulses it was changed from 10 to 15.





**Figure (4.2, a): FESEM image of ZnS thin film deposited on glass substrate with 15 laser pulses, laser pulse energy of 100 mj and repetition rate of 2 Hz**

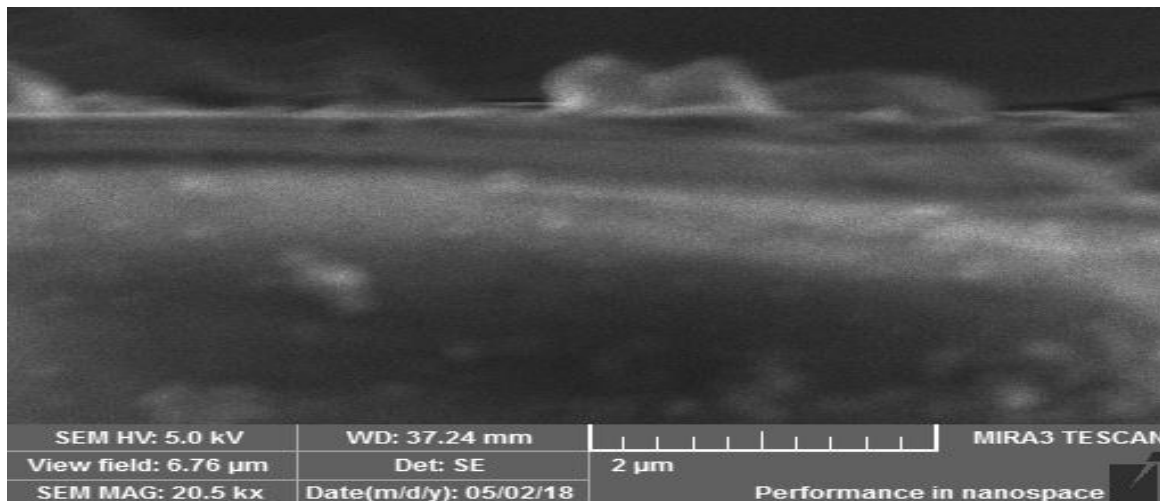
Figure (4.2, b) shows the FESEM image of the thickness measurement of the ZnS deposited on glass substrate when the number of laser pulses was 15.



**Figure (4.2, b): FESEM image of thickness size measurement of ZnS thin film deposited on glass substrate with 15 laser pulses, laser pulse energy of 100 mj and repetition rate of 2 Hz**

Compare to the figure (4.1, b) which shows the FESEM image of the thickness measurement of the ZnS thin film figure (4.2, b) showed that when the number of laser pulses increase the thickness of the ZnS deposited thin film is increased.

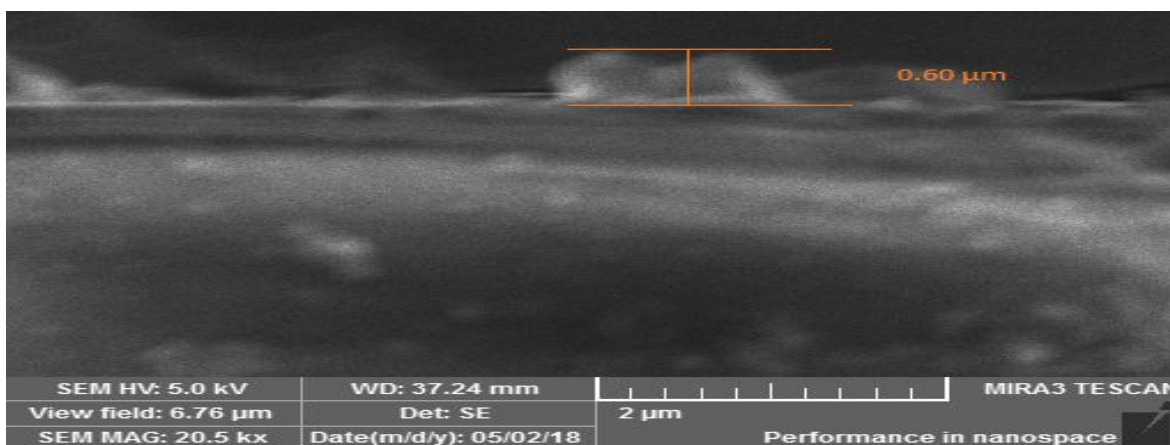
When the number of laser pulses is changed to 20 while the other deposition parameters were kept fixed as in previous situation, the deposited ZnS thin film imaged using field emission scanning microscope machine as shown in figure (4.3, a).



**Figure (4.3, a): FESEM image of ZnS thin film deposited on glass substrate with 20 laser pulses, laser pulse energy of 100 mj and repetition rate of 2 Hz**

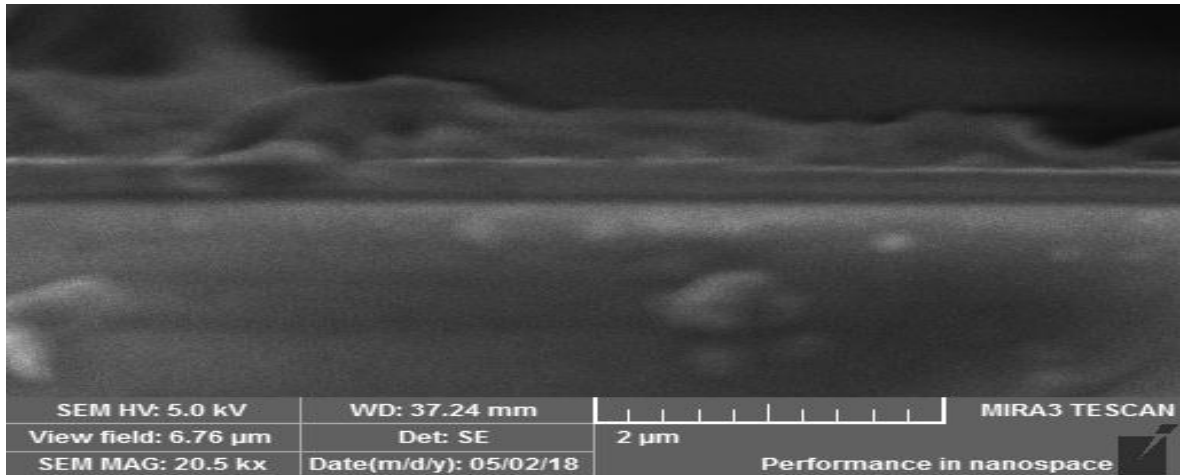
The deposited ZnS thin film thickness shown in figure (4.3, a) is high dense and has a non smooth surface when compared to the previous thin film samples that obtained with 10 and 15 number of laser pulses.

Figure (4.3, b) below shows the FESEM image of the deposited ZnS thin film when the number of laser pulses was 20.



**Figure (4.3, b): FESEM image of thickness size measurement of ZnS thin film deposited on glass substrate with 20 laser pulses, laser pulse energy of 100 mj and repetition rate of 2 Hz**

Again figure (4.3, b) support the idea that increasing the number of laser pulses result in an increase in the thickness of the deposited ZnS thin film. Finally we use 25 number of laser pulses to deposit ZnS thin film sample, using the same other deposition parameter (laser pulse energy of 100 mj, pulse repetition rate of 2 Hz, and the target to substrate distance and angle of 2 cm and 45°, respectively) and the deposited ZnS thin film examined using the FESEM and its image was shown in figure (4.4, a).



**Figure (4.4, a): FESEM image of ZnS thin film deposited on glass substrate with 25 laser pulses, laser pulse energy of 100 mj and repetition rate of 2 Hz**

The FESEM image of the thickness measurement of the ZnS thin film deposited using 25 number of laser pulses is shown in figure (4.4, b).

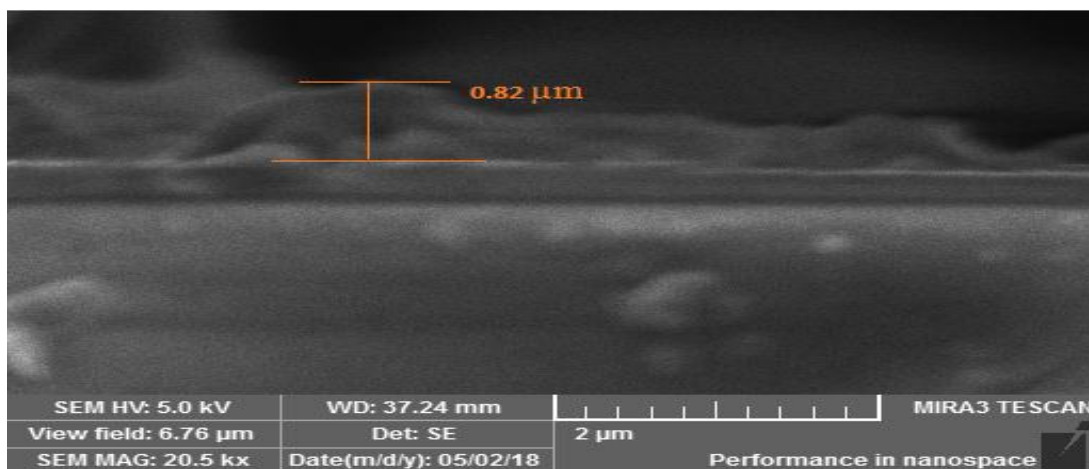


**Figure (4.4, b): FESEM image of thickness size measurement of ZnS thin film deposited on glass substrate with 25 laser pulses, laser pulse energy of 100 mj and repetition rate of 2 Hz**

It's now clearly that increasing the number of laser pulses while other pulse laser deposition parameters remains fixed result in increase of the thickness of the ZnS deposited thin films. Now to investigate how the numbers of laser pulses influence the thickness of the ZnS deposited thin films. The measured thickness and the corresponding number of laser pulses used for deposition are tabulated in table (4.1).

**Table 4.1: Thicknesses of the four fabricated ZnS thin films versus number laser pulses:**

Number of laser pulses	ZnS thin film thickness in ( $\mu\text{m}$ )
10	0.32
15	0.42
20	0.60
25	0.82

The above result of the thickness of the ZnS thin films and the number of laser pulses used for the deposition is plotted in figure (4.5).

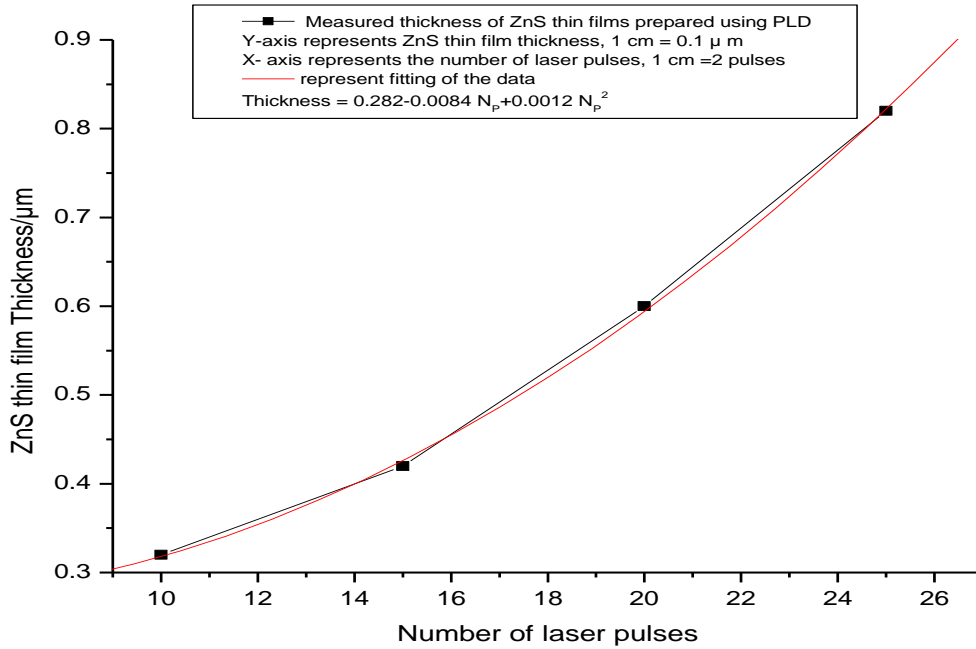


**Figure (4.5): The ZnS thin film thicknesses versus the number of laser pulses used for deposition**

Clearly as figure (4.5) shows, the relation between the number of laser pulses and the thickness of the deposited ZnS thin film is a nonlinear one.

The measured film thickness and the transmission data recorded for each ZnS thin film were used calculate the refractive indices using equation (3.1) and absorption coefficients using equation (3.2) and for each ZnS thin film at the laser wavelengths. For each laser wavelength the transmission intensities before and after the deposition of the ZnS thin films were recorded and the transmission percentage was calculated as  $(T\% = I_t/I_o)$  for The ZnS thin films tabulated in table (4.2) and then plotted for each ZnS thin film as shown in figure (4.6).

**Table 4.2: Transmission percentages at certain wavelengths for four ZnS thin films**

$\lambda$ (nm)	T % for $S_1$	T% for $S_2$	T% for $S_3$	T% for $S_4$
532	0.62	0.6	0.55	0.50
632.8	0.6	0.55	0.57	0.49
660	0.58	0.58	0.52	0.46
675	0.59	0.54	0.50	0.44
820	0.57	0.52	0.49	0.43
915	0.54	0.53	0.46	0.41

Note that R can be found as  $R=1-T$ ,

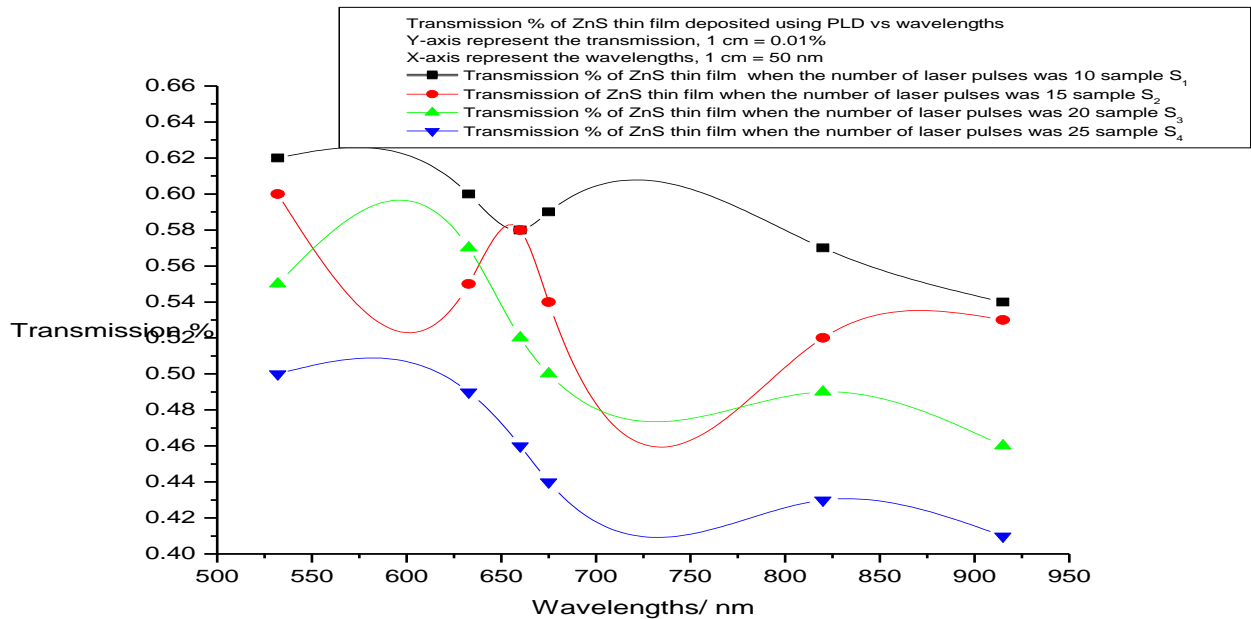


**Figure (4.6): Transmission spectra of the four ZnS thin film samples deposited using different number of laser pulses**

Figure (4.6) shows the transmission percentage ( $T\% = I_t/I_o$ ) at a certain laser wavelengths for the four ZnS thin film samples  $S_1$ ,  $S_2$ ,  $S_3$ ,  $S_4$  deposited using (10, 15, 20, and 25) number of laser pulses respectively. It's clearly that from figure (4.6) for each ZnS thin film and at each laser wavelength the transmission percentage is unique, moreover, the transmission of the sample  $S_1$  deposited using a 10 number of the laser pulses of thickness  $0.32 \mu\text{m}$  is high than the transmission of the other ZnS thin films of the highest thicknesses. Also figure (4.6) shows that the transmission of each ZnS thin film becomes lower as the wavelength increased.

The refractive indices are calculated for each ZnS thin film using equation (3.1) at certain wavelengths and tabulated in table (4.3), and then plotted in figure (4.7).

**Table 4.3: Refractive indices of the four ZnS thin film samples deposited with different number of laser pulses:**

$\lambda$ (nm)	n for $S_1$	n for $S_2$	n for $S_3$	n for $S_4$
532	2.51	2.58	2.58	2.95
632.8	2.58	2.76	2.75	2.99
660	2.65	2.65	2.65	3.13
675	2.61	2.79	2.95	3.22
820	2.69	2.87	2.99	3.27
915	2.8	2.83	3.13	3.38

Figure (4.7) shows the refractive indices of the four ZnS thin film samples ( $S_1$ ,  $S_2$ ,  $S_3$ , and  $S_4$ ).

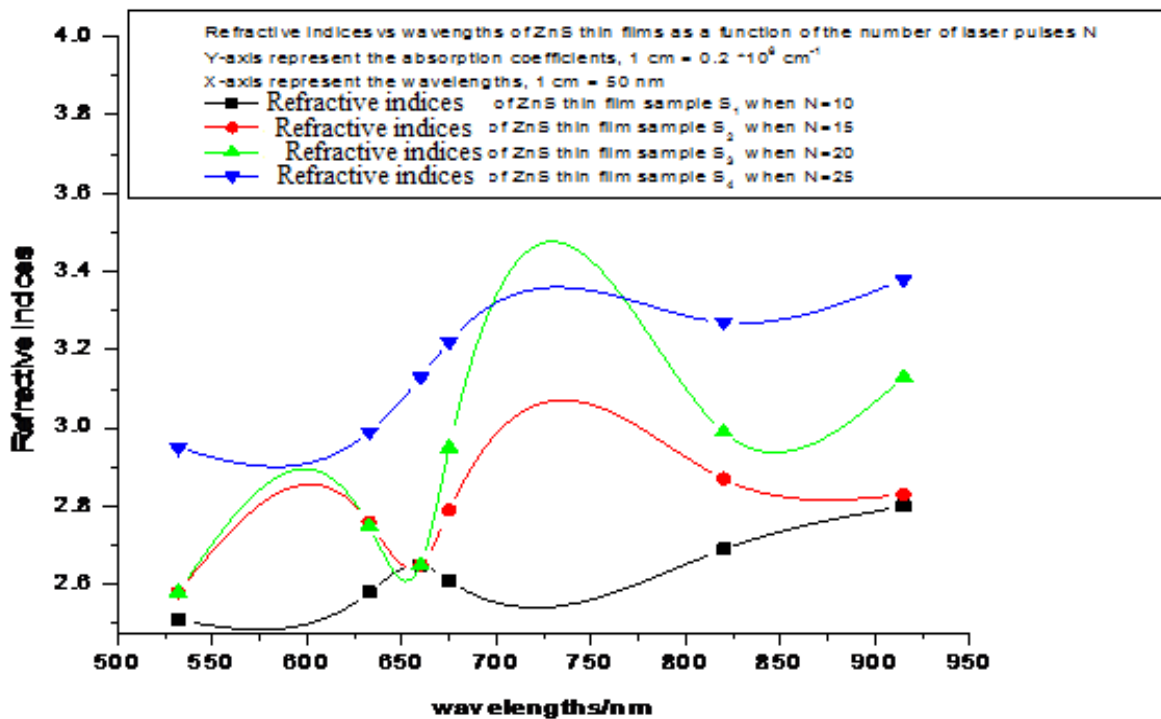


**Figure (4.7): The refractive indices of the four samples of ZnS thin films versus wavelengths as a function of the number of laser pulses**

Figure (4.7) showed that the refractive indices of the ZnS thin film is depending on its thickness and it vary with wavelength.

As shown in figure (4.7) the highest values of the refractive indices are of that of ZnS thin film sample  $S_4$  which of high thickness and which deposited with 25 number of laser pulses.

The absorption coefficients of the ZnS thin film four samples deposited using (10, 15, 20 and 25) number of the laser pulses were calculated from the transmission data and the measured film thicknesses and tabulated in table (4.4) and is plotted in figure (4.8).



**Table 4.4: Absorption coefficients of the four ZnS thin film samples deposited with different number of laser pulses:**

$\lambda$ (nm)	$\alpha$ ( $\text{cm}^{-1}$ ) * $10^3$ for $S_1$	$\alpha$ ( $\text{cm}^{-1}$ ) * $10^3$ for $S_2$	$\alpha$ ( $\text{cm}^{-1}$ ) * $10^3$ for $S_3$	$\alpha$ ( $\text{cm}^{-1}$ ) * $10^3$ for $S_4$
532	28.287	20.857	13.383	8.902
632.8	27.375	19.119	13.870	8.724
660	26.646	20.161	12.653	8.190
675	26.918	18.771	12.166	7.834
820	26.006	18.076	11.923	7.656
915	24.637	18.423	11.193	7.300

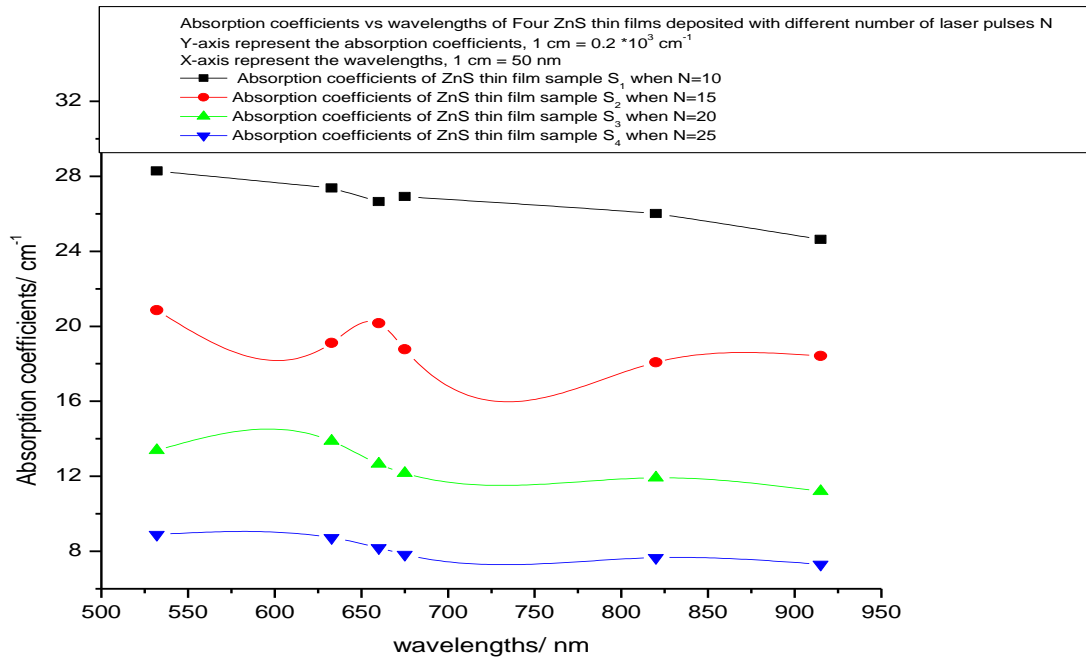
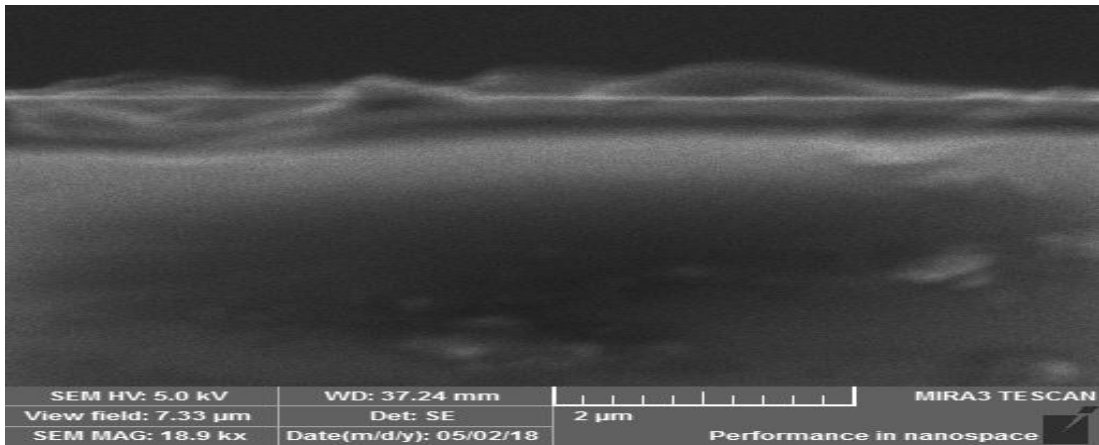


**Figure (4.8): Absorption coefficients versus wavelengths for four samples of ZnS thin films as a function of the number of laser pulses**

The absorption coefficients of the pulsed laser deposited ZnS thin films varies with thickness and for each thickness the absorption coefficients is unique as shown in figure (4.8). Also the absorption coefficients of the ZnS sample S<sub>1</sub> which is deposited using 10 number of laser pulses and of the smallest thickness (0.32 micrometer) has the highest values for all laser wavelengths and this is due to the fact that the absorption coefficients has the reciprocal of the dimension of the thickness.

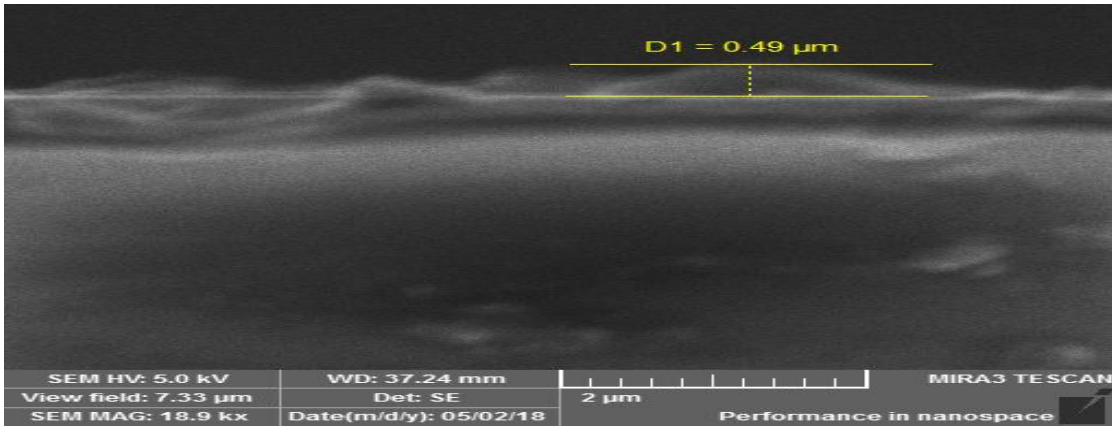
### **4-3 Effect of Pulse Energy on the thickness and Optical properties of ZnS thin films:**

For the case of the effect of pulse energy on the optical properties of ZnS thin films, four ZnS thin films using 20 laser pulses with pulse repetition rate of 5 Hz and varying pulse energies of (125, 150, 175, and 200) mj were deposited on glass substrates. Figure (4.9, a) shows the FESEM image of the ZnS thin film deposited when the pulse energy was 125 mj, while the pulse repetition rate, the number of the laser pulses was 20, and the target to substrate distance and angle were 2 cm, and 45°, respectively.



**Figure (4.9, a): FESEM image of ZnS thin film deposited on glass substrate with laser pulse energy of 125 mj and repetition rate of 5 Hz**

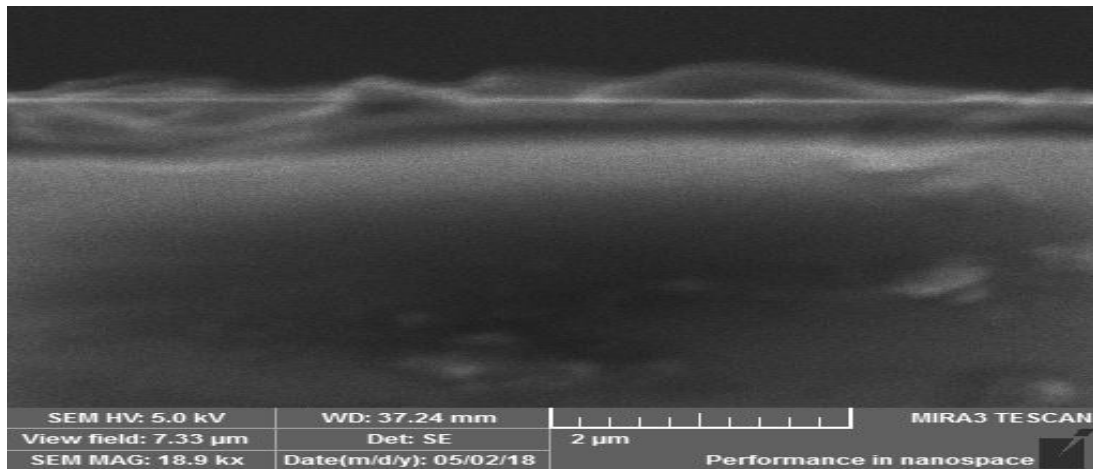
The FESEM image of the thickness measurement of these ZnS thin film is shown in figure (4.9, b).



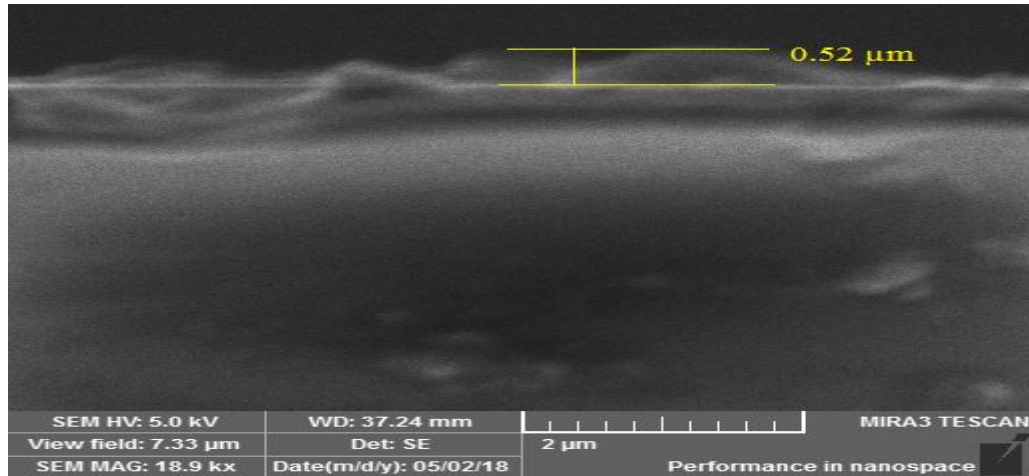
**Figure (4.9, b): FESEM image of thickness size measurement of ZnS thin film deposited on glass substrate with laser pulse energy of 125 mj and repetition rate of 5 Hz**

The ZnS thin film thickness as shown in the above image was 0.49 microns.

All laser parameters such as the laser wavelength, pulse repetition rate, and the number of the laser pulses were kept fixed as the previous and the only varied pulse parameter was the laser pulse energy, a 150 mj is used instead of 125 mj. The FESEM image of deposited ZnS thin film in this case is shown in figure (4.10, a).



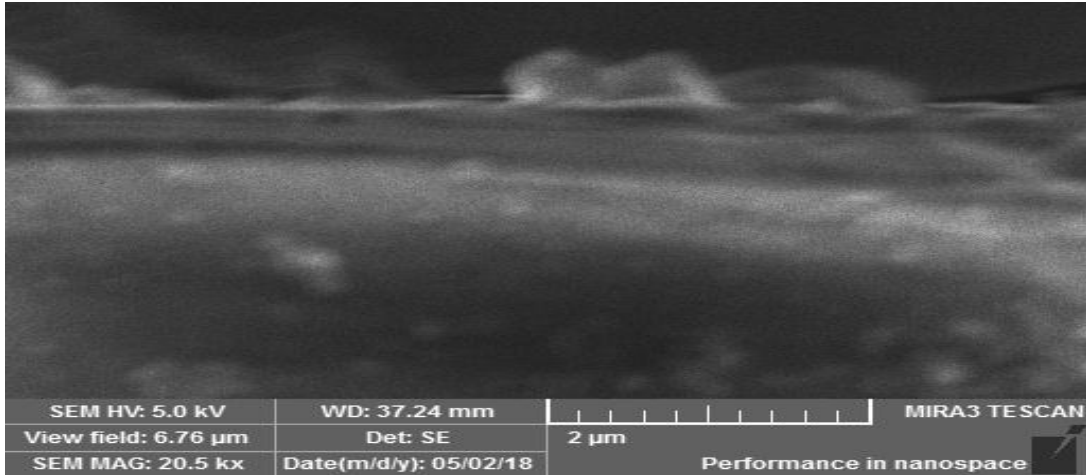
**Figure (4.10, a): FESEM image of thickness measurement of ZnS thin film deposited on glass substrate with laser pulse energy of 150 mj and repetition rate of 5 Hz**



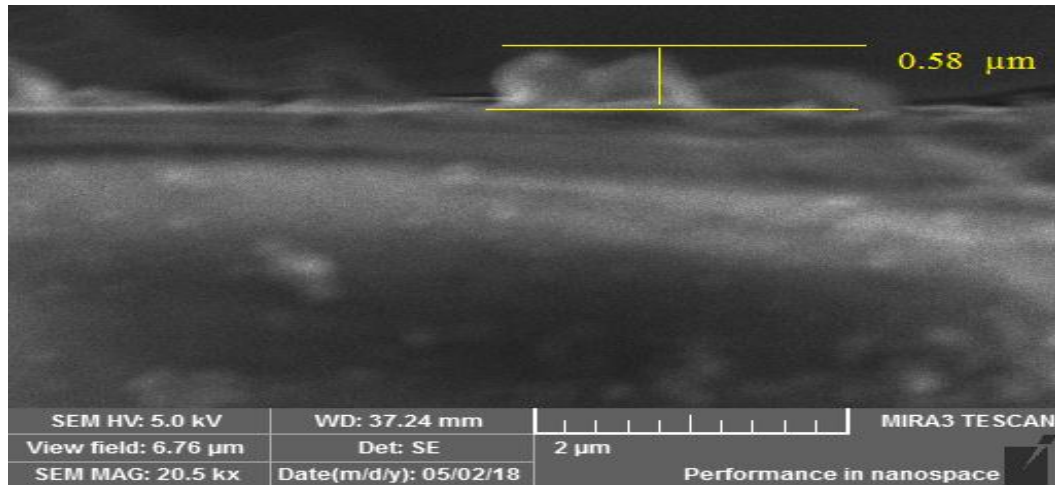
**Figure (4.10, b): FESEM image of thickness size measurement of ZnS thin film deposited on glass substrate with laser pulse energy of 150 mj and repetition rate of 5 Hz**

Again as shown in figure (4.10, b) the thickness of the deposited ZnS thin film when the laser pulse energy was measured using the FESEM measurement tool, and it was shown to be 0.52 microns which is large than that obtained when the laser pulse energy was 125 mj.

Figures (4.11, a) and (4.11, b) shows the FESEM image of the deposited ZnS thin film and the FESEM image of its thickness measurement, respectively, when the laser pulse energy is 175 mj while 5 Hz of pulse repetition rate and 20 number of laser pulses is used. In addition to target to substrate distance and angle of 2 cm and 45° respectively, are used as the deposition condition of these ZnS thin film on glass substrate.



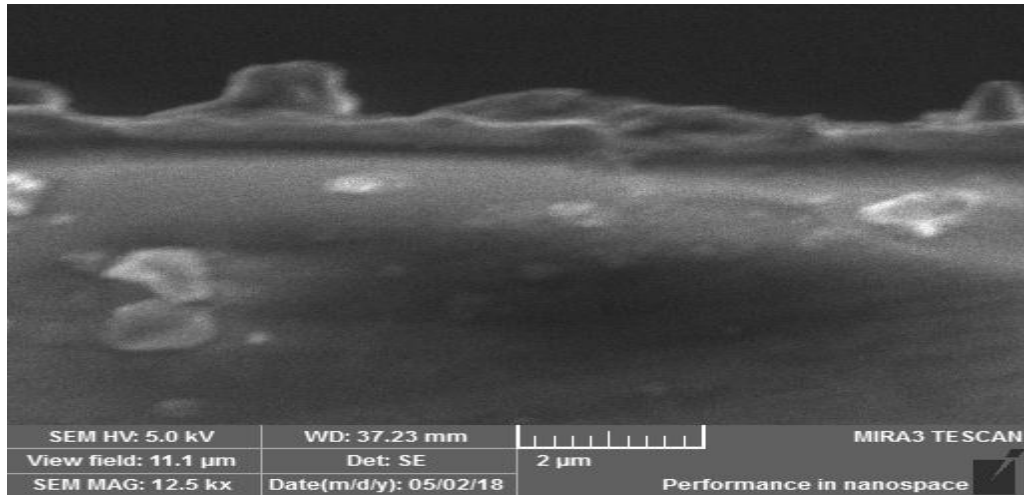
**Figure (4.11, a): FESEM image of thickness measurement of ZnS thin film deposited on glass substrate with laser pulse energy of 175 mj and repetition rate of 5 Hz**



**Figure (4.11, b): FESEM image of thickness size measurement of ZnS thin film deposited on glass substrate with laser pulse energy of 175 mj and repetition rate of 5 Hz**

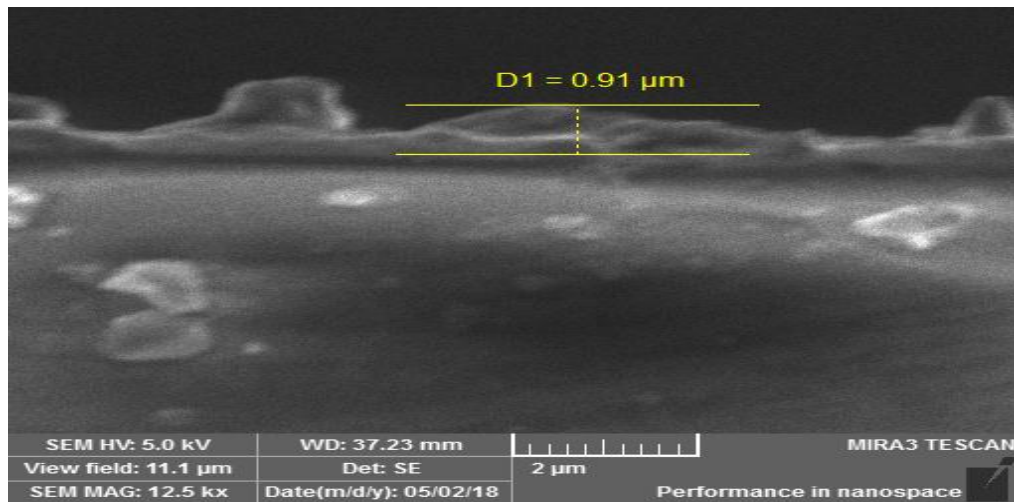
As compared to the two previous ZnS thin films obtained with 125 mj and 150 mj, the ZnS thin film deposited when the pulse energy is 175 mj is of largest thickness among the two and has a non uniform thickness distribution.

Figure (4.12, a) shows the ZnS thin film when the laser pulse energy was increased to 200 mj, while the same deposition conditions is used.



**Figure (4.12, a): FESEM image of thickness measurement of ZnS thin film deposited on glass substrate with laser pulse energy of 200mj and repetition rate of 5 Hz**

The measurement of the thickness of the ZnS thin deposited when the pulse energy is 200 mj was shown in figure (4.12, b).



**Figure (4.12, b): FESEM image of thickness size measurement of ZnS thin film deposited on glass substrate with laser pulse energy of 200 mj and repetition rate of 5 Hz**

As shown in figure (4.12, b) the film thickness was 0.91 micron when the pulse energy was 200 mj. The laser pulse energy ZnS thin film thickness relation is tabulated in table (4. 5) which is plotted in figure (4.13).

**Table (4.5): Laser pulse energy against ZnS thin film thickness**

Pulse Energy in (mj) with R.R =2 Hz	ZnS thin film thickness in ( $\mu\text{m}$ )
125	0.49
150	0.52
175	0.58
200	0.91

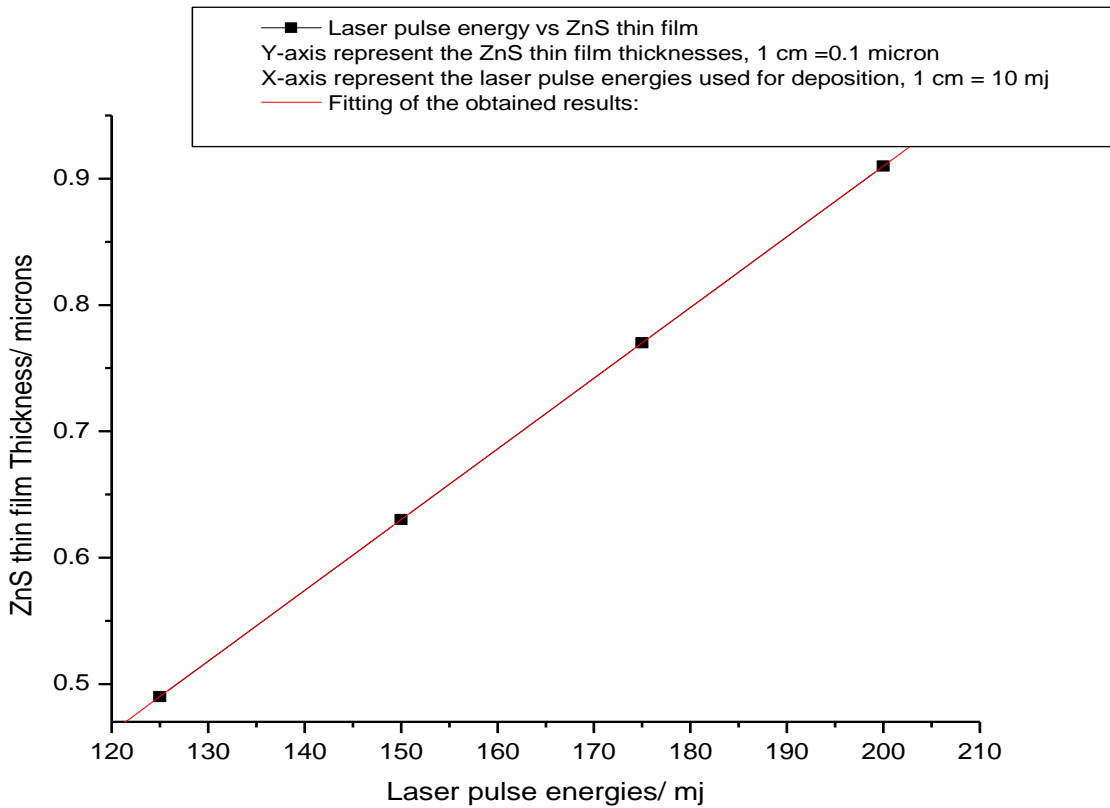


**Figure (4.13): The relation between laser pulse energy ZnS thin film thickness**

From figure (4.13) it is clear that increasing the pulse energy results in an increment of the ZnS thin film thickness. Again as done with the previous samples of the ZnS thin

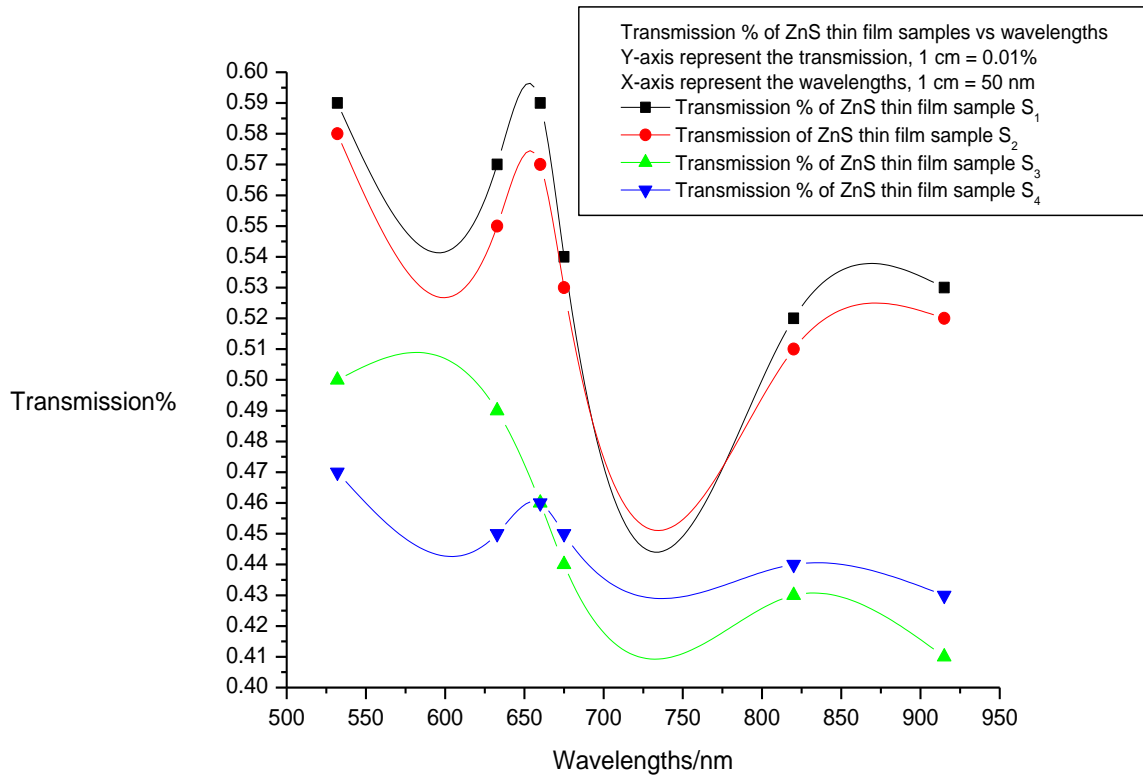
films deposited using different number of laser pulses, the transmission data were recorded and used together with the measured ZnS thin film thicknesses to calculate their optical properties (refractive index and absorption coefficients) at certain wavelengths. Table (4.6) shows the transmission of the four ZnS thin film using the transmission intensities of the wavelengths before and after the deposition (according to  $T\% = I_i/I_o$ ).

**Table (4.6): Transmission of the four ZnS thin films deposited using different laser pulse energy:**

$\lambda$ (nm)	T % for S <sub>1</sub>	T% for S <sub>2</sub>	T% for S <sub>3</sub>	T% for S <sub>4</sub>
532	0.59	0.58	0.50	0.47
632.8	0.57	0.55	0.49	0.46
660	0.58	0.57	0.46	0.45
675	0.54	0.53	0.44	0.45
820	0.52	0.51	0.43	0.44
915	0.53	0.52	0.41	0.43

The transmission of the four ZnS thin films deposited using different laser pulse energy table (4.7) is plotted in figure (4.14).





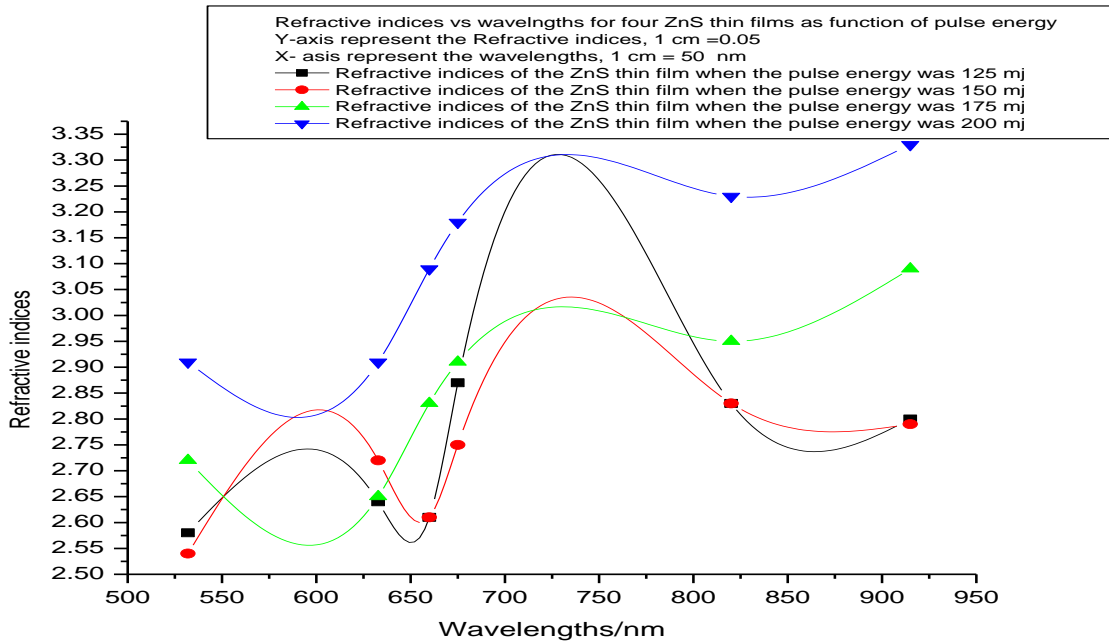
**Figure (4.14): Transmission spectra of the four ZnS thin film samples deposited using different laser pulse energy**

Figure (4.14) showed that the thickness of the thin film affected its transmission, comparing between the transmission of the four samples of ZnS thin films, samples  $S_1$ ,  $S_2$ ,  $S_3$ , and  $S_4$  together with the results shown in figure (4.13) illustrates that the large thickness of the thin film and thus the higher the pulse energy used for deposition gives the lower transmission of the film.

The relation between the calculated refractive indices for the four samples of ZnS thin films deposited on glass substrates using pulsed laser technique with fixed pulse repetition rates and varied pulse energy and were done according to equation (3.1x) tabulated in table (4.7), and are plotted as a function of wavelengths as shown in figure (4.15).

**Table (4.7): Refractive index of the four ZnS thin films deposited using different laser pulse energy:**

$\lambda$ (nm)	n for S <sub>1, 0.49</sub>	n for S <sub>2, 0.52</sub>	n for S <sub>3, 0.58</sub>	n for S <sub>4 0.91</sub>
532	2.58	2.54	2.72	2.91
632.8	2.64	2.72	2.65	2.91
660	2.61	2.61	2.83	3.09
675	2.87	2.75	2.91	3.18
820	2.83	2.83	2.95	3.23
915	2.80	2.79	3.09	3.33



**Figure (4.15): Refractive indices of the four ZnS thin film samples deposited using different laser pulse energy**

The absorption coefficients of the ZnS thin films deposited using different pulse energy were calculated according to equation (3.2) was tabulated in table (4.8) and is plotted in figure (4.16).

**Table 4.8: Absorption coefficients of the four ZnS thin film samples deposited using different laser pulse energy:**

$\lambda$ (nm)	$\alpha$ ( $\text{cm}^{-1}$ ) * $10^3$ for S <sub>1</sub>	$\alpha$ ( $\text{cm}^{-1}$ ) * $10^3$ for S <sub>2</sub>	$\alpha$ ( $\text{cm}^{-1}$ ) * $10^3$ for S <sub>3</sub>	$\alpha$ ( $\text{cm}^{-1}$ ) * $10^3$ for S <sub>4</sub>
532	18.061	17.307	14.224	7.989
632.8	17.448	15.865	14.741	7.244
660	17.755	16.730	13.627	7.582
675	16.530	15.576	12.931	7.834
820	15.918	15.000	12.672	7.252
915	16.224	15.288	11.896	6.758

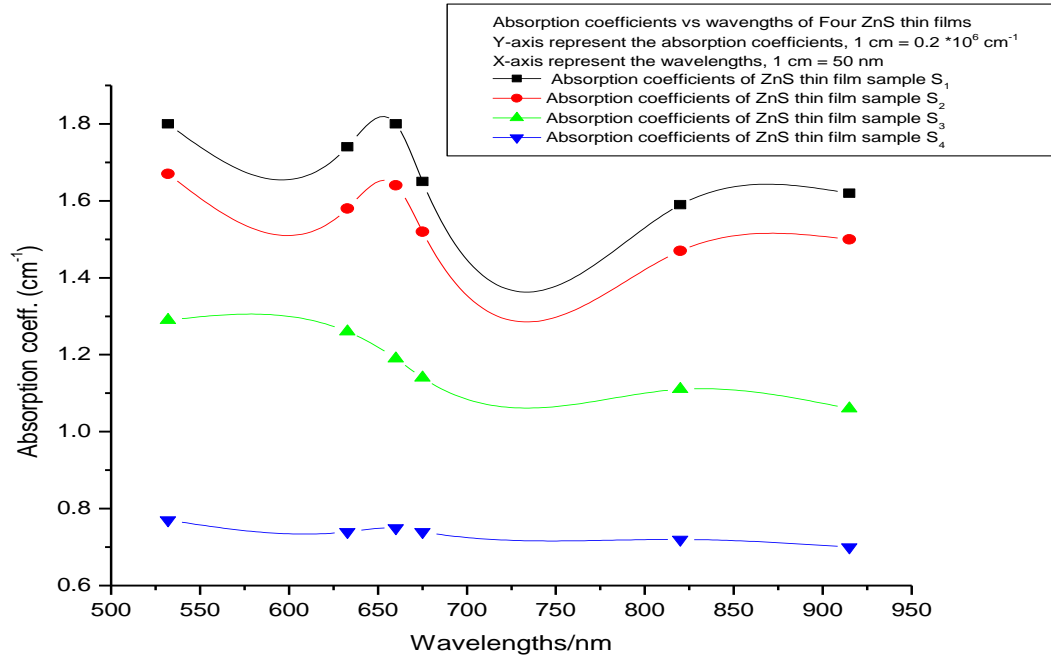


**Figure (4.16): Absorption coefficients versus wavelengths for four samples of ZnS thin films deposited using different pulse energy**

The absorption coefficients of the ZnS thin films for all samples showed in figure (4.16) exhibits similar shape with the wavelengths for samples 1 and 2 deposited using 125 and 150 mj pulse energy and that is due to the approximately equal thickness (0.49 and 0.52) microns, but for the other two ZnS samples the behaviour of the absorption coefficients with the wavelengths is totally different due to high difference in their thickness from the first two. Therefore, as evident from the results shown in figure (4.16) the absorption coefficients of the pulsed laser deposited ZnS thin films varies with thickness.

#### **4-4 Discussion:**

Figures (4.1, a and b) to (figures 4.4, a and b) showed that four ZnS thin films samples deposited on glass substrate by pulse laser deposition method successfully. Using Q-switched Nd: YAG laser source with wavelength 1064 nm, pulse repetition rate of 2 Hz, laser pulse energy of 100 mj, the target to substrate distance and angle of 2 cm, and 45°, respectively, and the only varied deposition parameter between the four ZnS thin films is the number of laser pulses. And it is clear that when comparing the measured thickness of the obtained thin films as correspondence to the number of laser pulses, the higher the number of pulses give the higher the ZnS thin film thickness, also as comparison between the figures the 25 number of pulses give the higher and the non-uniform in the thickness distribution as compared with that obtained with low number of pulse 10 for example as shown figure (4.1, a). One clearly concluded that the number of laser pulses influence the growth (thickness increased as the number of laser pulses increase) and the optical properties of the ZnS thin films this agree with work of ( Eman Nasir in 2013).

The effect of laser pulse energy on the growth of ZnS thin films showed in figures (4-6, a) through (4-10, a) illustrate that the morphology of the Zinc sulfide thin films is highly dependent on the pulse energy used, and figures (4-6, b) through (4-10, b) proved that increasing the pulse energy results in an increment of the thickness of the deposit. The transmission of the all samples of fabricated ZnS thin film in the region from 532 to 915 nm showed in figure (4-12) and figure (4-15) prepared using different number of laser pulses and different laser pulse energies were in the range from (0.41-0.60) % and these results is in good agreement with the work of Bushra A. Hasan and Eman M. Nasir (2015).The transmission spectra of all ZnS samples are in good agreement with the work of K. R. Murali in the region from 532 nm to 915 nm. Also it was shown that the transmission of all ZnS thin films is large for visible wavelengths

than that of wavelengths in the IR region and this also agrees with the work of (Dr. Kadhim Abid Hubeatir, 2015). It was observed that the refractive index,  $n$  increase on increasing the film thickness and this is in good agreement of the work carried by (E. Marquez in 2014).

The overall assessment of this work is that the thickness of the deposited ZnS thin films was found to be linearly dependent on the pulse energy and nonlinearly dependent on the number of laser pulses used. The transmission spectra in the tested region (532 to 915) nm were found to be in the range from (0.41 to 0.62) % depending on the ZnS thin film thickness, and for each ZnS thin film the transmission spectrum is unique. The refractive indices of all samples were determined; and for each sample and it were found to be change with wavelength, the highest refractive index was obtained for the sample of the smallest thickness 0.49 microns. The absorption coefficients were found to be varied from (28.287 to 7.300)  $\times 10^3 \text{ cm}^{-1}$  and the results obtained were in very good agreement with the literature.

## 4-5 Conclusions:

The following points concluded this work:

- In this study, the effect of the of laser parameters (laser pulse energy and number of pulses (while pulse repetition rate, and target to substrate distance and angle were kept fixed) on the thickness and optical properties of ZnS thin films deposited on glass substrate by pulse laser deposition method has been studied.
- The thickness of the ZnS thin films was measured using the FESEM measurement tool, and the transmission spectra of the deposited ZnS thin films at certain laser wavelengths were recorded.
- The relation between the pulse energy and the ZnS fabricated films was found to be linear and that of the number of laser pulses and the thickness of the fabricated ZnS thin films was nonlinear one.
- Optical properties (refractive indices, and absorption coefficients) of the fabricated ZnS thin films were calculated.

In conclusion ZnS thin films deposited by pulse laser deposition technique can be used to produce optical components in the range from visible to IR regions by controlling its thickness via controlling the number of laser pulses.

## **4-6 Recommendation:**

The following are recommended for future work:

- Further researches on the pulse laser deposition of thin films of sulphur compounds are recommended
- Using pulsed laser technique to fabricate multi-layer of ZnS thin films.
- Study the effect pulse repetition rate on the thickness and optical properties of thin films.
- Study the effect of using different substrate types and annealing on thickness and optical properties of ZnS thin films.
- Study the effect of target to substrate distance and angle on the properties of laser deposited ZnS thin films.
- Using the PLD technique to fabricate thin films and apply them in dye-sensitized solar cell (DSSC).
- Study other properties of the fabricated ZnS thin films such as thermal, electrical and so on.



## References:

Alessia Sambri, (2008), Pulsed laser deposition of complex transition metal oxides: plume expansion and film growth,( PhD thesis, Physics Department, Universita di Napoli Federico II, Italy), downloaded from website: [http// fisica.unica.it](http://fisica.unica.it), 2/8/2017

A. U. Ubale, K.S. Chipade, and M .V. Bhute et al. (2012), Structural, Optical and Electrical Properties of Nanostructured CdS:CuS Composite Thin Films Grown by CBD Method, *International Journal of Materials and Chemistry*, [DOI: 10.5923/j.ijmc.20120204.09], volume 2, issue 4, pp. 165-172

Bushra A.Hasan and Eman M. Nasir (2015), Structural Morphology and Electrical Properties of Vacuum Evaporated SnS Thin Films, *International Journal of Current Engineering and Technology*, Vol.5, No.2, pp. 910-917

C. R. IORDĂNESCU et al., (2017), CHARACTERIZATION OF CdS-DOPED GLASS FILMS OBTAINED BY PULSED LASER DEPOSITION, *Romanian Journal of Materials* , **47 (1)**, 60 – 65

Dina Atoyán (2006), characterization of thin-film zinc telluride on glass prepared by low-temperature nanosecond pulsed-laser deposition, (M.Sc. thesis- Graduate College of Bowling Green, State University website, Ohio)

D. Benetti, R. Nouar, R. Nechache, and H. Pepin et al., (2017), Combined magnetron sputtering and pulsed laser deposition of TiO<sub>2</sub> and BFCO thin films, *nature, SCIENTIFIC RepoRts*|7:2503, PMC5451404, PMID: 28566679

Đekić M et al. (2017), Influence of deposition parameters on pulsed laser deposition of K<sub>0.3</sub>MoO<sub>3</sub> thin films, *Bulletin of the Chemists and Technologists of Bosnia and Herzegovina*, volume 48, pp.1-4, 2017

Donald L. Smith (1995), *Thin- Film Deposition*, edition, McGraw Hill, USA, New York

Eman M. Nasir, (2013), Fabrication and Characterization of n-ZnS/p-Si and n-ZnS:Al/p-Si Heterojunction, *International Journal of Engineering and Advanced Technology (IJEAT)*, Volume-3, Issue-2, December 2013, pp.425-429

E. Ma´rquez, E. R. Shaaban, and A. M. Abousehly, Structural and optical properties of ZnS thin films, *International Journal of New Horizons in Physics*, volume 1, issue 1, pp. 17-24

E. Chen (2004), Thin Film Deposition II, Erli Chen Fabrication II, (lecture notes, Harvard University, downloaded from: <http://www.mrsec.harvard.edu>, 17/9/2017)

Hameed, M. A. (2015), Physical Properties of Nanostructured Silicon Dioxide Prepared by Pulsed-Laser Deposition, *Journal of Physical Vapor Deposition Science and Technology*, Volume 9, Issue 10, October 2015, pp. 451-454

Hans-Ulrich Krebs, Martin Weisheit, Michael Buback, and Joerg Faupel, (2003), Pulsed Laser Deposition (PLD) -A Versatile Thin Film Technique, *Advances in Solid State Physics*, volume 43 , 505-518, pp.101-107

Zexian Cao (ed.), Thin Film Growth, , chapter in Thin Film Growth Physics Material Sciences and Applications by Y. Kajikkawa Woodhead publishing SERIES IN Electronics and Optical Materials, (2011), pp.60-82

Kasturi Chopra (2012), Thin Film Device Applications, Springer, ISBN-10:146133683X

Khadher AL-Rashdi<sup>1</sup>, Mazahar Farooqui, Mohammad Mohsin , Gulam Rabbani, METAL OXIDE THIN FILMS: AMINI REVIEW, *Journal of Advanced Scientific Research*, , *J Adv Sci Res*, 2016, 7(1): 01-08, ISSN: 0976-9595

Kumar V, Saroja M., Venkatachalam M, and Shankar S (2015), Synthesis and characterization of ZnS thin films by Sol-gel and dip spin coating methods, *International of Recent Scientific Research*, volume 6, issue 11, pp. 7377-7379

K. R. Murali (2014), Optical properties of pulse electrodeposited ZnS films, *IOSR Journal of Applied Physics (IOSR-JAP)*, Volume 6, Issue 3 Ver. II, pp. 9-14

Krishna Seshan (ed.), HANDBOOK OF THIN-FILM DEPOSITION PROCESSES AND TECHNIQUES: Principles, Methods, Equipment and Applications, second edition, (2002), Noyes Publications, Norwich, New York, U.S.A.

Mahdi Hasan Suhail and Raoof Ali Ahmed (2014), Structural, optical and electrical properties of doped copper ZnS thin films prepared by chemical spray pyrolysis technique, *Advances in Applied Science Research*, volume 5, issue 5, pp. 139-147

MA Sangamesha, K. Pushpalatha, G. L. Shekar, and d S. Shamsundar , (2013), Preparation and Characterization of Nanocrystalline CuS Thin Films for Dye-Sensitized Solar cells, *ISRN Nanomaterials*, Volume 2013, Article ID 829430, 8 pages

Microscopy - MATERIAL SCIENCE - Electron Microscopy – Tescan, MIRA3, [online] available from <https://www.wirsam.com/product/mira-3>, visited, 16/2/2018

Michael N. R. Ashfold, Frederik Claeysens Gareth M. Fuge and Simon J. Henley, Pulsed laser ablation and deposition of thin films, *Chemical Society Reviews*, issue 1, 2004

Nafie A. Almuslet, Kh. M. Haroun, and Yousif H. Alsheikh (2018), Pulse Energy Effect on the Optical Properties of Pulse Laser

Deposited SiO<sub>2</sub> Thin Films, International Journal of Trend in Scientific Research and Development (IJTSRD), Volume – 2, Issue – 6, Sep – Oct 2018, pp. 47-54

Nafie A. Almuslet and Yousif H. Alsheikh (2015), Investigation of the Optical Properties of Liquid Deposition CuSO<sub>4</sub> Thin Film, *IJSRST*, Volume 1, issue 5, pp. 132-136

Nadeem M. Y., Waqas Ahmed, and Wasif M. F., ZnS THIN FILMS – AN OVERVIEW, *Journal of Research (Science)- Bahauddin Zakariya University*, Multan, Pakistan, Vol.16, No.2, October 2005, pp. 105-112 , ISSN:1021-1012

NORITAKE-ELEC.COM, (2015), Thin Film Technology, [online] available from: <http://noritake-elec.com/technology/core-technology/thin-film-technology>, visited 2:2/2017

Oriental Wison (2017) , 1320/1064/532 nm Q-switched Nd: YAG laser, Model Name OW-D, product datasheet, Beijing Oriental Wison Mechanical & Electronic Co., Ltd, China.

Rao M.C. (2014), Technological Applications of Thin Films in Functional Materials, *Journal of Environmental Science, Computer Science and Engineering & Technology, JECET*; Sc.D.Vol.3.No.3, pp. 1645-1652, E-ISSN: 2278– 179X

Robert Eason (ed.), (2007), PULSED LASER DEPOSITION OF THIN FILMS, APPLICATIONS-LED GROWTH OF FUNCTIONAL MATERIALS, WILEY-INTERSCIENCE A JOHN WILEY & SONS, INC.

Rik Greoenen, Jasper (2017), Synthesis and Characterization of CuInS<sub>2</sub> Thin Film for Photoelectrochemical Application, (PhD thesis, Department of Physics, Avinashilingam Deemed University For Women), India , downloaded from: [shodhganga.inflibnet.ac.in](http://shodhganga.inflibnet.ac.in), 31/ 12/2018

R. Maity and K.K. Chattopadhyay (2004), Synthesis and optical characterization of ZnS and ZnS: Mn nanocrystalline thin films by chemical route, *Nanotechnology*, volume 15, issue 7, pp. 812 – 816

Schneider, C. W., and Thomas Lippert (2010), chapter five: Laser Ablation and Thin Film Deposition, *Laser Processing of materials: Fundamentals, Applications and development*, [online], available at <http://www.psi.ch/materials/BooksEN/christof-book.pdf>, downloaded: 16 May 2018

Shimadzu hand press machine, product information (P/N 200-64174), Shimadzu Corporation, Japan 2013

Tamil Ilakkiya J (2017), Synthesis and Characterization of CuInS<sub>2</sub> Thin Film for Photoelectrochemical Application, (PhD thesis- Department of Physics, Avinashilingam Deemed University For Women), downloaded from: [shodhganga.inflibnet.ac.in](http://shodhganga.inflibnet.ac.in), 31/ 12/2018, India

Tatiana E. Itina, Jorg Hermann, Philippe Delaporte, and Marc Sentis, 2002, Laser-generated plasma plume expansion: Combined continuous-microscopic modeling, *PHYSICAL REVIEW E* 66, 066406, The American Physical Society, pp.1-12.

Thomasnet.com, Thin Film Deposition Coating, [online] available from [http://Thomasnet.com/articles/chemicals/Thin\\_Film\\_Deposition\\_Coating](http://Thomasnet.com/articles/chemicals/Thin_Film_Deposition_Coating), visited 17/9/2017

Thomas Lippert (2012), Deposition and Characterization of Thin Films, from: <http://www.lipert.ch>, visted 2018

V. A. Goldade, L. S. Pinchuk, A. V. Makarevich, and V.N. Kestelman (2005), Plastic for Corrosion Inhibition, Springer series in Material science, Verlag Berlin Heidelberg.

V. Timoshevskii, Y Ke, H Gu, and D Gall, The influence of surface roughness on electrical conductance of thin Cu films: An ab initio study, *Journal of applied Physics*, volume 103, issue 11, pages 113705, AIP, [Pdf] available from: <http://www.semantic scholar.org>

Y.L. Wang, G.I. Albokhary, X.C. Ding et al. (2016) , Evolution of the Collision Rate in the Process of Propagation of Laser Generated Plume into an Inert Gas, *Armenian Journal of Physics*, vol. 9, issue 2, pp. 130-137

Yousif Hassan Alsheikh Abd Alraheim, (2018), Study the Optical Properties of Silicon Dioxide Thin Films Prepared Using Q-Switch Nd:YAG Laser Deposition, (PhD thesis), Sudan University of Science & Technology

## Appendices:

### **American Journal of Modern Physics 2018; 7(5): 173-179**

<http://www.sciencepublishinggroup.com/j/ajmp> doi: 10.11648/j.ajmp.20180705.11 ISSN: 2326-8867 (Print); ISSN: 2326-8891 (Online)

### **Effect of Pulse Energy on the Optical Properties of ZnS Thin Films Prepared Using Pulse Laser Technique**

Khalid Mohammed Haroun<sup>1</sup>, **Mohammed Nouman Mohammed Abdalla**<sup>2</sup>, Sohad Saad Elwakeel<sup>2</sup>,  
Yousif Hassan Alsheikh Abd Alraheim<sup>3</sup>

**Abstract:** In these work four samples of ZnS thin films deposited on glass substrate using pulse laser deposition method with different pulse energies, the effect of the laser pulse energy on the optical properties of the four ZnS thin films fabricated was studied. Q-Switched Nd: YAG laser with the fundamental wavelength 1064 nm, laser Pulse energies of (125, 150, 175, and 200) mj with fixed number of pulses of 20, and pulse repetition rate of 5 Hz were used. The target to the substrate distance and angle were kept fixed. The film thicknesses were measured using FESEM measurement tool. The thickness of the deposited ZnS thin films was found to be linearly dependent on the pulse energy used. The transmission spectra in the tested region (532 to 915) nm were found to be in the range from 0.41 to 0.59% depending on the ZnS thin film thickness, and for each ZnS thin film the transmission spectrum is unique. The refractive indices of all samples were determined; and for each sample and it were found to change with wavelength, the highest refractive index of 5.6 at 915 nm was obtained for the sample of the smallest thickness 0.49 microns. Transmission spectra, absorption coefficients and the refractive indices they were in good agreement with the literature.

**Keywords:** Laser Pulse Energy, Optical Properties, ZnS Thin Films, Pulse Laser Deposition (PLD)

**Number of Laser Pulses Influence on Optical Properties of Pulse Laser  
Deposited ZnS Thin Films**

**Mohamed N.M. Abdalla<sup>1</sup>, Yousif H. Alsheikh<sup>2</sup>, Kh. M. Haroun<sup>3</sup>, and Sohad S. Elwakeel<sup>1</sup>,**

**ABSTRACT:**

In present work four samples of ZnS thin films deposited on glass substrate using pulse laser deposition method with different number of laser pulses, the effect of the number of laser pulses on the optical properties of ZnS thin films was studied. Q-Switched Nd: YAG laser with the fundamental wavelength 1064 nm, laser pulse energy of 100 mj with fixed pulse repetition rate of 2 Hz were used, and varied number of (10, 15, 20 and 25) pulses . The target to the substrate distance and angle were kept fixed. The film thicknesses were measured using FESEM measurement tool. Thickness of the deposited ZnS thin films was found to be dependent on the number of laser pulses used. The transmission spectra in the region (532 to 915) nm were recorded and was showed that for each ZnS thin film the transmission spectrum is unique. The refractive indices of all samples were determined. Transmission percentage were found to be varied from (0.4 to 0.62) %, absorption coefficients were found to be varied from (28.287 to 7.300) \*10<sup>3</sup> cm<sup>-1</sup> and the refractive indices, depending on the film thickness and the wavelength were in very good agreement with the literature.

**Keywords:** pulse laser deposition, number of pulses, optical properties, ZnS thin films